[American Journal of Science, Vol. 309, October, 2009, P. 661–688, DOI 10.2475/08.2009.02]

REACTANT-PRODUCT TEXTURES, VOLUME RELATIONS, AND IMPLICATIONS FOR MAJOR-ELEMENT MOBILITY DURING NATURAL WEATHERING OF HORNBLENDE, TALLULAH FALLS FORMATION, GEORGIA BLUE RIDGE, U.S.A.

MICHAEL A. VELBEL*†, ANGELA R. DONATELLE*,
and MICHAEL J. FORMOLO**

ABSTRACT. Natural weathering of hornblende from the Tallulah Falls Formation (Georgia, U.S.A.) takes place under thoroughly leached, oxidizing conditions. At the earliest stage of weathering, corrosion of hornblende forms denticulated terminations, with only minimal porosity apparent within the partially pseudomorphic kaolin-group weathering product or between it and the reactant mineral. Isovolumetric replacement of hornblende by kaolin-group clay or precursor products implies inheritance of parent-mineral silica tetrahedra by the weathering products and largely immobile behavior of Si during early weathering. Aluminum, normally considered immobile or minimally mobile during weathering, must be imported into early-stage weathering products. More advanced weathering of hornblende forms denticulated terminations, separated from the earlier-formed products by a large, continuous peripheral void; porosity is much more conspicuous at this stage. Late-stage ferruginous products precipitate from Fe mobilized in solution. Dissolved Fe to form the late-stage goethite can be entirely derived from the parent hornblende, requiring only short transport distances for aqueous Fe between the source parent mineral and the location of product precipitation. Textural and volumetric relationships between naturally weathered hornblende and its partially pseudomorphic weathering products suggest structurally controlled immobility of much parent-mineral Si and considerable mobilization of Al at early stages of weathering, but at more advanced stages of weathering the textural and volumetric relationships are consistent with immobility of Al and Fe and leaching of substantial Si and all base cations.

Key words: Weathering, Kinetics, Mafic-ultramafic, Amphibole, Hornblende

INTRODUCTION

The purpose of this paper is to address mineral-scale weathering phenomena that influence the relative mobilities of the three major cations—Si, Al, and Fe—in Earth's crust during weathering of ferromagnesian chain-silicate minerals. The weathering of primary host-minerals of these elements, the formation of secondary-mineral host-phases, and the mobilities of these elements influence regional and global geochemical cycles on short and protracted timescales.

Chain-silicates are the dominant ferromagnesian minerals, constituting 16 percent of Earth's crust (Klein, 2002). Most naturally occurring chain-silicates belong to the pyroxenes (single-chain silicates) and amphiboles (double-chain silicates) (Klein, 2002). Ferromagnesian silicate minerals play an important role in global and regional geochemical cycles (Wilson, 2004). Globally, Mg-silicates (pyroxene, amphibole, biotite, chlorite and olivine) as a group weather more rapidly than any Ca-, Na- or K-silicates (Lerman and others, 2007), and weathering of Mg-silicates is ultimately responsible for delivering 50 to 75 percent of the world's dissolved riverine Mg^{2+} flux (Berner and Berner, 1996; Lerman and others, 2007). More than half of the silicate weathering contribution is from Ca- and Mg-silicates (Lerman and others, 2007), with

* Department of Geological Sciences, 206 Natural Science Building, Michigan State University, East Lansing, Michigan 48824-1115 U.S.A.
** Max-Planck-Institut für Marine Mikrobiologie, Celsiusstraβe 1, D-28359 Bremen, Germany
† Corresponding author: velbel@msu.edu

35 percent from Ca-silicates (including calcic plagioclase, pyroxene, and amphibole), and 41 percent from Mg-silicates (including pyroxene, amphibole, biotite, chlorite, and olivine) (Berner and Berner, 1996). Chemical weathering of continental silicate-dominated lithologies is responsible for approximately 50 percent of the carbonic acid consumption (Berner and Berner, 1996; Lerman and others, 2007). Because carbonic acid is formed from atmospheric carbon dioxide through the intermediary soil atmosphere, weathering of Ca- and Mg-silicates (including the ferromagnesian silicates emphasized here) is a major geologic control on the sequestration of carbon dioxide in the long-term global geochemical carbon cycle throughout geologic time (Berner, 2004, 2006). Furthermore, the weathering of Ca- and Mg-silicates, including ferromagnesian silicates of this study, accounts for approximately 50 to 75 percent of the CO_2 consumption by continental processes (Berner and Berner, 1996; Lerman and others, 2007). Ferromagnesian silicates also contribute significantly to regional (smaller-than-global-scale) geochemical budgets. This is well illustrated by small-watershed studies of solute fluxes and the role of mineral weathering rates in natural mitigation of environmental acidity (for example, acid rain; Bricker and Rice, 1989).

The majority of literature discussing the role of ferromagnesian silicates and their weathering in regional and global geochemical cycling involves those minerals occurring as the ferromagnesian-silicate portion of felsic rocks. This is illustrated by published studies of mineral-weathering contributions to surface-water solute loads and fluxes. Although a few such studies emphasized (meta-)mafic rock types (for example, greenstone metabasalt, Katz and others, 1985; Katz, 1989; Rice and Bricker, 1995; amphibolite, Velbel, 1992), more small-watershed and regional solute studies examined watersheds on landscapes dominated by felsic rocks (Bricker, 1986; Bricker and Rice, 1989; O'Brien and others, 1997) or dominantly felsic parent rock types with minor mafic-mineral content (Miller and Drever, 1977; Newton and April, 1982; April and Newton, 1983a, 1983b, 1985; April and others, 1986; Hornung and others, 1986; Drever and Hurcomb, 1986; Dethier, 1988; Rochette and others, 1988; Psenner, 1989; Stauffer, 1990a, 1990b; White and others, 1998). There is less literature on the contributions of mafic-ultramafic rocks to regional and global solute geochemistry (Katz and others, 1985; Katz, 1989; Velbel, 1992; Rice and Bricker, 1995), and consequently the role of these rock types remains less well understood.

Many weathering and dissolution phenomena of common amphiboles are nearly identical to those of common pyroxenes (Wilson, 2004; Velbel, 2007). Secondary minerals vary among different geochemical and leaching environments; aqueous geochemists (Tardy, 1971) and regolith geoscientists (Taylor and Eggleton, 2001) use a classification based on the major clay minerals that form. At early stages of weathering and/or under conditions of minimal leaching of dissolved products, 2:1 clay-minerals form as weathering products; such weathering, forming products comprising two tetrahedral silicate sheets per octahedral sheet, is termed *bisiallitic*. Intermediate degrees of weathering and/or leaching intensity lead to the formation of 1:1 clay-minerals; such weathering, forming products comprising one tetrahedral silicate sheet per octahedral sheet, is termed *monosiallitic*. When weathering has been so extensive or intense that silica has been completely leached from the weathering profile, hydroxides and oxyhydroxides of Al are abundant and/or dominant weathering products; such weathering is termed *allitic*.

Textural relationships and patterns of elemental mobility vary with the formation of different weathering products of chain-silicates under different conditions. Previous work has examined textures and elemental mobility in early stages of bisiallitic weathering and advanced stages of monosiallitic weathering, but previous examinations of early stages of monosiallitic weathering are lacking. This study explores the consequences of the textural and compositional reactant-product relationships for

elemental mobility during hornblende weathering. These relationships between naturally weathered hornblende and its monosiallitic weathering products under thoroughly leached, oxidizing conditions place quantitative constraints on the active chemical weathering mechanisms and associated elemental mobility during hornblende weathering.

The weathering behavior of Al, saprolite Si/Al ratios, and solute HCO_3^-/Si ratios associated with weathering of mafic-ultramafic rocks deviate more from expectations of regional weathering behavior based on solute chemistry than any other rock type examined to date. For example, Gardner (1992) showed that Si:Al ratios in modern surface water solutes in deeply weathered landscapes are much higher than the Si:Al loss-ratios implied by the bulk chemical compositions of weathering profiles on the same landscapes. This implies greater loss of Al from the analyzed solids than can be accounted for by observed surface-water solutes, and the discrepancy is greatest for mafic-ultramafic rocks (Gardner, 1992). Schroeder and others (2000) found that solutes in groundwaters in weathered mafic rocks are more similar to the groundwaters in adjacent felsic rocks than would be expected from the elemental losses implied by the bulk chemical compositions of the weathered mafic solids. In order to address discrepancies and observed deviations in Si-Al behavior in saprolite and solutes associated with the weathering of high-grade metamorphic mafic parent materials similar to those studied by Gardner (1992) and Schroeder and others (2000), this study examines natural weathering of hornblende from an amphibolite unit near the Georgia-South Carolina border. The specific emphasis of this study is the relationships among reactant-product textures and the mobility of Si, Al, and Fe during monosiallitic/allitic chemical weathering of hornblende in mafic rocks like those that exhibit unexpected mobility patterns of these elements (Gardner, 1992; Schroeder and others, 2000).

Study Area: Bedrock Geology, Petrology, Structure

The amphibolite examined in this study is from the Tallulah Falls Formation, in the Tugaloo terrane (Hatcher and others, 2005) of the southern Appalachian Blue Ridge of northeastern Georgia (U.S.A.) (Helms and others, 1987). Bedrock in the area consists predominantly of amphibolite facies metasedimentary schists and gneisses, with local pods of mafic-ultramafic lithologies (Hatcher and others, 1984, 2005). The metasedimentary Tallulah Falls Formation is Late Precambrian in age (Hatcher, 1976), and was metamorphosed to amphibolite-facies conditions (Hatcher and others, 1984) during the Taconic orogeny (Hatcher and others, 2005).

Regolith in the study area is similar to the regolith developed on similar mafic parent rock types from which anomalous geochemical results have previously been reported (Gardener, 1992; Schroeder and others, 2000). Taylor and Eggleton (2001) provide a pragmatic definition that begins: "*Regolith* is all the continental lithospheric materials above fresh bedrock . . ." (Taylor and Eggleton, 2001, p. 3). The weathered *in situ* component of regolith called *saprolite* was defined by Becker (1895) as "thoroughly decomposed, earthy, but untransported rock." Saprolites are residual weathered material developed on crystalline parent rocks in which some or all of the primary minerals have been extensively weathered *in situ* to weathering products (Velbel, 1985a; Taylor and Eggleton, 2001).

Saprolite preserves textures and fabrics of the parent rock through the replacement of specific primary minerals by specific weathering products (Velbel, 1990; Nahon, 1991; Delvigne, 1998; Taylor and Eggleton, 2001). Where a weathering product replaces a euhedral parent mineral, the common term *pseudomorph* is appropriately used. When the parent mineral was anhedral, the alteration product has outlines that do not mimic crystal faces of the primary mineral. Delvigne (1998) introduced the term *alteromorph* to distinguish replacement of anhedral primary minerals from true

pseudomorphic replacement. Partial (rather than complete) replacement of primary minerals by alteration products at grain boundaries and fractures is common during silicate weathering. Septa of secondary minerals mark where grain boundaries and fractures used to be (Delvigne, 1998); the septa surround cavities where unreplaced primary mineral (subsequently removed leaving behind void space) used to be (Velbel, 1989; Delvigne, 1998). Such partial replacement, in which former fractures are preserved as products and former unreplaced parent-mineral remnants are now preserved as voids, was referred to as a "negative pseudomorph" or (in the case of Fe-bearing material) "ferruginous microboxwork" by Velbel (1989). However, in the more systematic textural classification of Delvigne (1998), such features are termed *septo-alteromorphs*. See Taylor and Eggleton (2001) and Delvigne (1998) for more detailed discussion about the terminology of naturally weathered materials at field and petrographic scales, respectively.

Results are reported here for a small corestone collected from an extensively weathered saprolitic regolith developed on amphibolite of the Tallulah Falls Formation immediately adjacent to the ultramafic core of the Laurel Creek Complex at Stop 2 of McSween and Hatcher (1985) (fig. 1). The specific Tallulah Falls Formation amphibolite lithology sampled is dominated by hornblende with only negligible gedrite. It resembles samples L-79 and L-112-N of the adjacent Laurel Creek Complex (Helms and others, 1987). Calcic amphibole in these samples ranges in composition from magnesio-hornblende and tschermakitic hornblende to ferroan pargasite (see amphibole nomenclature in Hawthorne and Oberti, 2007), and is referred to as hornblende throughout most of Helms and others (1987).

METHODS

The integration of corrosion and replacement textures, chemical composition of hornblende and product phases, and reactant-product molar-volume relationships permits testing of various hypotheses regarding elemental mobility during chain-silicate weathering. For mineral characterization, covered and uncovered polished petrographic thin sections were prepared and examined by optical petrography. Pieces of air-dried partially weathered Tallulah Falls Formation amphibolite were adhered to aluminum stubs, coated with Au, and examined in secondary electron imaging (SEI) mode using a JEOL T-20 scanning electron microscope (SEM) with a Polaroid camera in the Department of Geological Sciences at Michigan State University. Selected areas were re-examined in SEI mode with a JEOL 6400 SEM equipped with digital image acquisition and Noran and Oxford energy dispersive spectroscopy (EDS) systems at the Center for Advanced Microscopy at Michigan State University. SEI reveals the surface topography of the sample. Polished uncovered thin sections were examined in both SEI and backscattered electron imaging (BEI) mode on the same JEOL 6400 SEM/EDS systems. In BEI mode, contrast is determined by spatial variations in atomic number (Z). Imaged spots containing material with low average Z produce the weakest image signal and therefore the darkest shades (dark gray, black) and spots containing high average Z producing the strongest image signal and therefore the lightest shades (light gray, white). Both the reactant and product minerals in this study are silicates and oxides of major rock-forming elements and the element primarily responsible for Z-contrast variations is Fe. BEI of polished thin-sections allows the direct determination of relationships between SEM-scale textures and optical properties of the same objects, and enables examination of textural and compositional features beneath the surfaces examined by SEI.

For the determination of bulk clay mineralogy, two different lithologies of an extensively weathered portion of the hand sample were crushed and ultrasonically agitated. Oriented mounts of both the clay-size (<2 μm) fraction and the fine-silt sized fraction from each subsample were prepared using the filtration method of Drever

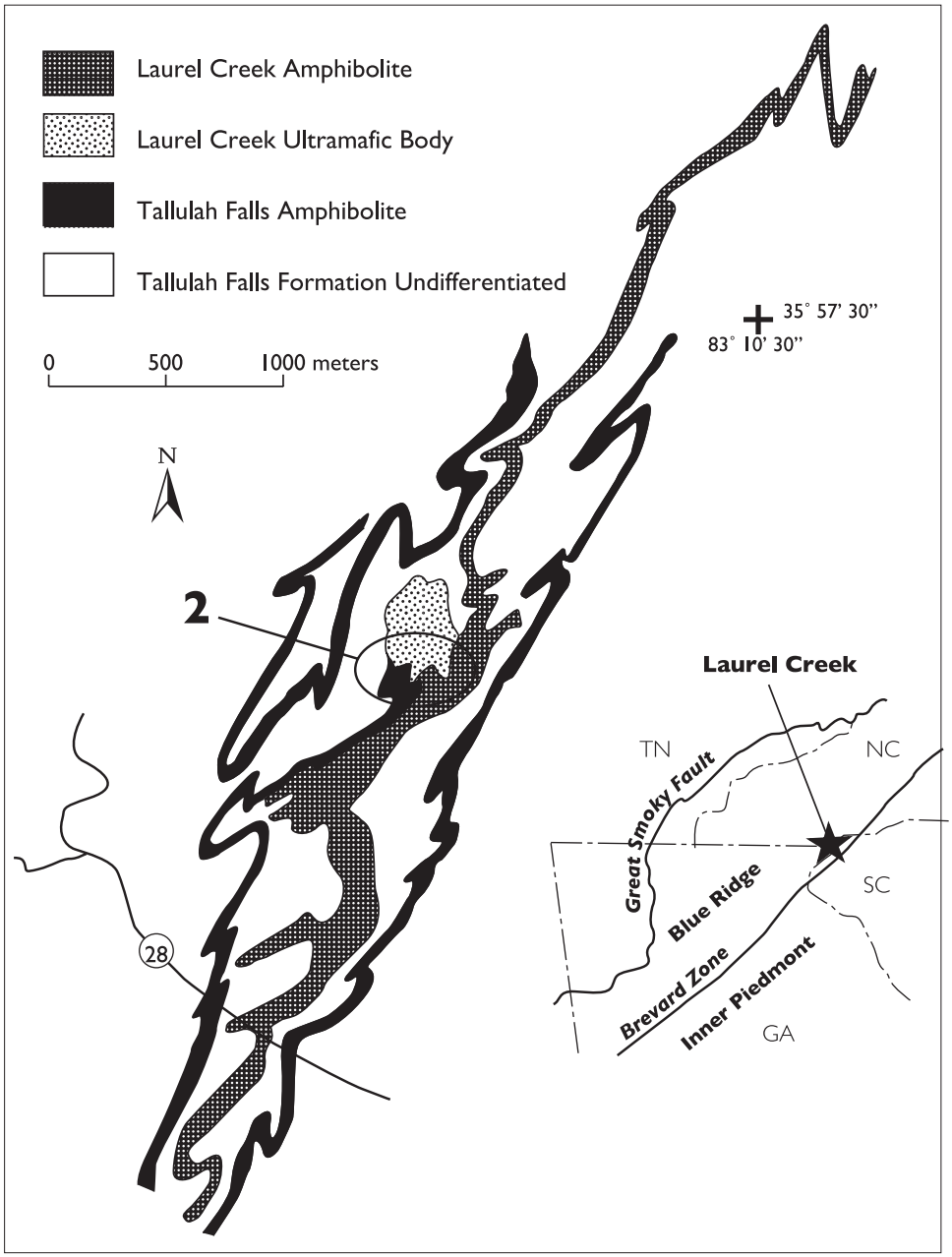

Fig. 1. Geologic map of the study area showing the sample location (field trip stop 2 of McSween and Hatcher, 1985). The sample examined for this study is from the Tallulah Falls Formation where it is tectonically juxtaposed against the Laurel Creek Complex in the local study area. Adapted from Helms and others (1987).

(1973) and Keller and others (1986). X-ray diffraction data (XRD) were acquired with a Philips APD (Automated Powder Diffraction) 3720 X-Ray diffractometer using Cu K-α radiation, equipped with an APD 3521 goniometer, a θ-compensating slit, a 0.2 mm

TABLE 1

Hornblende compositions used in this study

Formula	Source Table (and analysis) in Helms and others (1987)
$K_{0.001}Na_{0.340}(Na_{0.003}Ca_{1.658}Mn_{0.005}Fe_{0.334})(Fe_{1.302}Mg_{2.617}Ti_{0.037}Al_{1.045})(Si_{6.240}Al_{1.760})O_{22}(OH)_2$	2 (L-79)
$K_{0.001}Na_{0.271}(Na_{0.067}Ca_{1.618}Mn_{0.034}Fe_{0.282})(Fe_{1.199}Mg_{2.713}Ti_{0.042}Al_{1.046})(Si_{6.383}Al_{1.617})O_{22}(OH)_2$	2 (L-112-N)
$Na_{0.395}Ca_{1.628}Mg_{2.744}Fe_{1.421}Al_{2.744}Si_{6.446}O_{22}(OH)_2$	6
$Na_{0.2}(Ca_{1.9}Fe_{0.1})(FeMg_3Al)(Si_{6.8}Al_{1.2})O_{22}(OH)_2$	7 (L-112-N)
$Na_{0.4}(Ca_{1.9}Fe_{0.1})(Fe_{1.3}Mg_{2.9}Al_{0.8})(Si_{6.8}Al_{1.2})O_{22}(OH)_2$	7 (L-79)

receiving slit, and a graphite monochromater on the diffracted beam. Samples were scanned over a range of approximately 4 to 28° (some preparations were run to 38°) 2θ with a step size of 0.020° and a time per step of 4 s, resulting in a scan speed of 0.30° 2θ per minute.

Product-reactant molar-volume ratios (V_p/V_r) were calculated for the replacement of Tallulah Falls Formation hornblende by weathering products typical of thoroughly leached oxidizing weathering environments, specifically kaolinite and goethite (Velbel, 1989, 1993a). Calculations followed the approach of Velbel (1993a, eq. 2), who applied the Pilling-Bedworth relationship from metallurgy to silicate weathering under well-leached, oxidizing weathering conditions. Assuming element *e* is immobile during weathering (letting all of element *e* present in the reactant mineral be immobile and incorporated into the product mineral) the product-reactant volume ratio is given by

$$V_p/V_r = n_{e,r}V^o_p/n_{e,p}V^o_r \quad (1)$$

where $n_{e,i}$ is the stoichiometric subscript of element *e* in mineral *i*, and V^o_i is the molar volume of mineral *i* ($i = r$ for the reactant, p for the product). V_p/V_r is the volume of product mineral produced per unit volume of reactant mineral, if element *e* is immobile. Previous applications of this concept to silicate-mineral weathering investigated the potential for formation of transport-inhibiting ("protective") surface layers on Fe- and Al-bearing silicate minerals from the Fe and Al in those parent minerals under well-leached, oxidizing conditions (Velbel, 1993a).

Velbel (1989) and Velbel and Barker (2008) demonstrated that the molar-volume approach can also be used to investigate elemental mobility during mineral weathering and replacement. If the volume of product present is less than the volume predicted from the volume-ratio equation, then the element assumed to be immobile for the purposes of calculating the volume ratio has actually been depleted from the pseudomorph/alteromorph. If the volume of product present is greater than predicted, then the element has been imported into the pseudomorph/alteromorph. If the actual volume of product present is equal to that predicted, the observations are consistent with the assumption that the element used was immobile.

All molar volumes used in this paper are from the tabulation used by Velbel (1993a), except for hornblende, which is represented here by the molar volume of pargasite (274.94 cm^3/mol; Smyth and Bish, 1988). As shown below, hornblende compositions in the Tallulah Falls Formation and the Laurel Creek Complex at this locality (Helms and others, 1987) are very similar. From the range of compositions reported for similar hornblende from the adjacent Laurel Creek Complex by Helms and others (1987), stoichiometric extrema are chosen to calculate the full range of potential volumetric relationships for each reactant-product pair. Microprobe analyses of calcic amphibole (hornblende *sensu lato*) from Table 2 of Helms and others (1987) and slightly idealized (for modeling purposes; Helms and others, 1987) average stoichiometric and structural formulae for hornblende (from Tables 6 and 7 in Helms and others, 1987) are shown in table 1. These formulae define the total range of

TABLE 2

Volumes of kaolinite and goethite formed from a unit volume of hornblende assuming immobility of selected elements from hornblende

Reactant-product pair	Immobile element	Minimum $n_{e,r}$ Per $O_{22}(OH)_2$	Maximum $n_{e,r}$ Per $O_{22}(OH)_2$	V^o_p	$n_{e,p}$	V^o_r	Minimum V_p/V_r	Maximum V_p/V_r
Hbl-kaolinite	Si	6.24	6.8	99.236	2	274.94	1.13	1.23
	Al	2.0	2.81	99.236	2	274.94	0.361	0.506
Hbl-goethite	Fe	1.1	1.64	20.693	1	274.94	0.083	0.123

stoichiometric proportions of Si, Al and Fe in the reactant hornblende, shown in table 2. A simplified hornblende formula consistent with mid-range Si, Al and Fe abundances from Helms and others (1987) and table 2 of this paper is

$$Ca_2Fe_{1.4}Mg_3Al_{0.9}(Si_{6.5}Al_{1.5})O_{22}(OH)_2$$

However, for the volumetric calculations, the values used come from the range of stoichiometric subscripts taken from data tables in Helms and others (1987) and summarized here in table 2. For simplicity, stoichiometrically similar tschermakite,

$$Ca_2(Mg_3AlFe^{+3})(Si_6Al_2)O_{22}(OH)_2$$

(Hawthorne and Oberti, 2007) is used in writing reactions for illustrative purposes below.

RESULTS

In transmitted light, clinoamphiboles weather to secondary/tertiary minerals of various optical properties. The earliest stage of hornblende weathering preserved in this sample is shown in a backscattered electron image in figure 2. A high Z-contrast central parting is separated from denticulated hornblende terminations by symmetrically disposed low Z-contrast material. At more advanced stages of weathering, denticles are sufficiently well developed on hornblende remnants to be easily visible under the petrographic microscope (fig. 3). Figure 4 shows a backscattered electron image of a field-of-view similar to figure 3B, a doubly terminated denticulated hornblende remnant separated by a peripheral void from microboxwork structures that consist of ferruginous and clay-mineral weathering products.

Figure 5 is a backscattered electron image of a more advanced stage of weathering than figures 2–4. Figure 6 shows elemental maps of the field-of-view of figure 5. Ferruginous (high Z-contrast) product (a in fig. 5; conspicuous in the lower part of the Fe EDS map in fig. 6) marks the locus of a fracture originally transecting the hornblende crystal. Lower Z-contrast product occurs symmetrically disposed on either side of the fracture (b in fig. 5), leaving the first-formed (high Z-contrast) product as a central parting. At this more advanced stage of weathering, projections ("pendants" of Velbel, 1989; c in fig. 5) occur on the low Z-contrast material between the central parting and the dissolving hornblende. A typical denticulated hornblende remnant (d in fig. 5) is separated from the earlier-formed product by a peripheral void (e in fig. 5; Velbel, 1989, 2007; Proust and others, 2006). High Z-contrast product occurs on the product side (f in fig. 5) of the peripheral void. Elemental maps of Mg, Ca, Si, Al and Fe (fig. 6) show that high Z-contrast features in the backscattered electron image (the central parting, a in fig. 5, and the product lining the peripheral void, f in fig. 5) are Fe-rich, that low Z-contrast product (b and c in fig. 5) is richer in Si and Al, and that Mg and Ca are detectable in the denticulated hornblende remnant (d in fig. 5) but not detectable above background noise in any product.

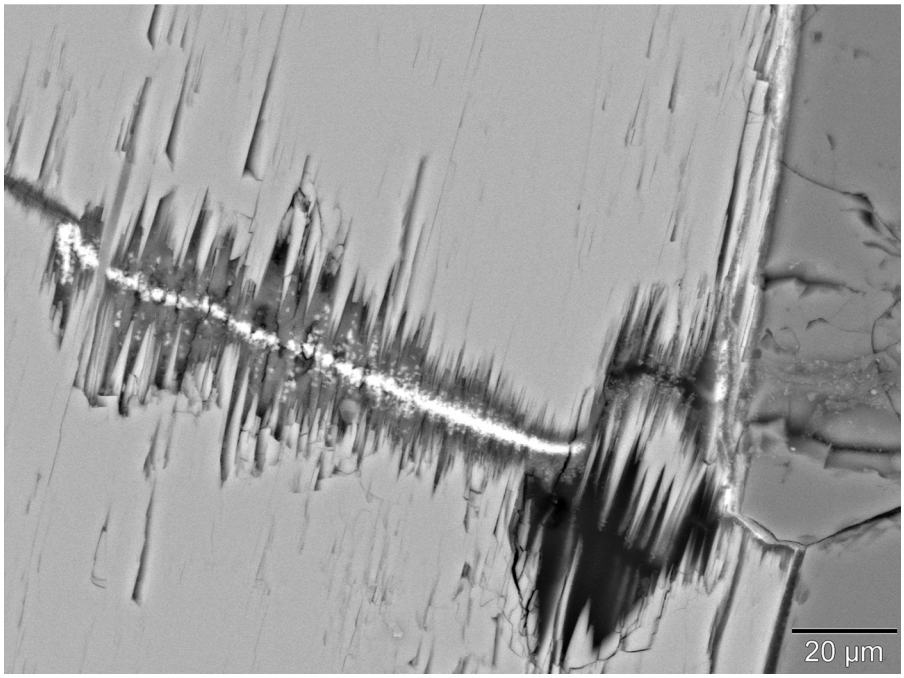

Fig. 2. Ferruginous (high Z-contrast) product marks locus of original fracture transecting hornblende crystal. Hornblende corrosion and replacement by lower Z-contrast product proceed symmetrically from the fracture, leaving the first-formed (high Z-contrast) product as a "central" parting (common in both serpentinization and weathering of chain-silicates; Velbel, 1989). Corrosion of hornblende forms typical denticulated termination (Velbel, 1989, 2007). Backscattered electron image.

Figure 7 shows representative X-Ray diffraction patterns of bulk fines (subdivided into $< 2\mu m$ and $> 2\mu m$ fractions). XRD analysis revealed peaks for common weathering products, including members of the 1:1 dioctahedral (aluminous) clay minerals (kaolin-halloysite group) (001) (0.706-0.736 nm), (110) (0.439 nm, asymmetric, as is common for tubular halloysite) and (002) (0.355 nm); goethite (110) (0.415 nm) and (111) (0.242 nm); and gibbsite (002) (0.485 nm). Some peaks attributable to primary minerals common in metamorphosed mafic rocks (for example, hornblende, anthophyllite, talc, quartz) and apatite (112) (0.278 nm) and (300) (0.268 nm) also occur in XRD patterns of some splits.

Figure 8 shows Mg-Fe-Ca and Al-Fe-Si ternary diagrams of EDS point analyses. Electron microprobe analyses of Ca-amphiboles in the adjacent Laurel Creek Complex (Helms and others, 1987) are shown for comparison. EDS analyses of the Tallulah Falls Formation hornblende are compositionally indistinguishable from the Ca-amphiboles in the adjacent Laurel Creek Complex reported by Helms and others (1987). EDS analyses of specific spots in septo-alteromorphic products associated with weathered hornblende (fig. 8B) reveal variable Fe contents; commonly, equal parts Si and Al; and low concentrations of Ca and Mg (see also fig. 6). Possible combinations of host minerals containing Si, Fe, and Al include kaolin-group minerals (including halloysite), gibbsite, goethite, and hematite. XRD identified minerals with d-spacings corresponding to a kaolin-group mineral, gibbsite and goethite. EDS spot analyses plotting on the join from Al:Si = 1:1 toward the Fe pole (fig. 8B) are therefore interpreted as coming from weathering products consisting of mixtures of a kaolin-group mineral and goethite (with minor gibbsite), intimately intermixed on a scale

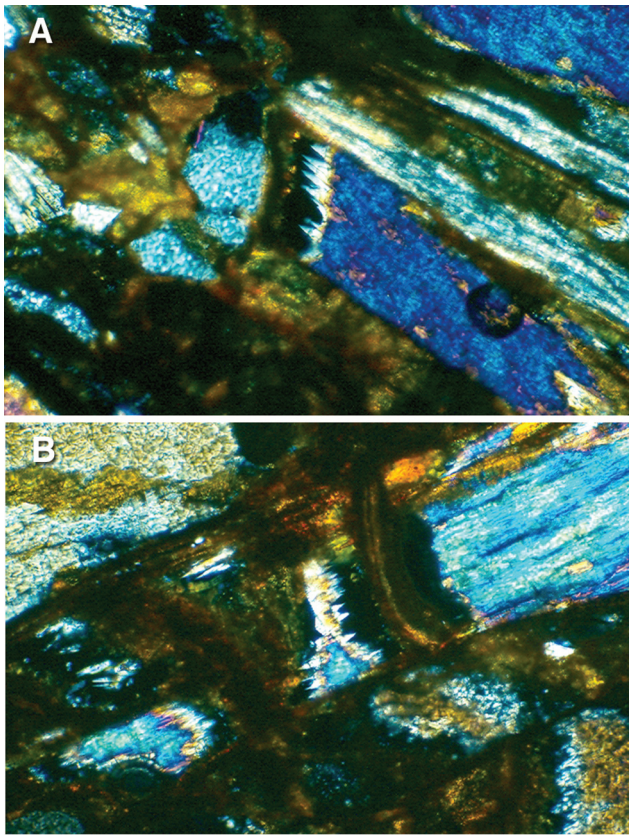

Fig. 3. Hornblende weathering features in thin-section. (A) Denticulated hornblende termination. (B) Doubly terminated denticulated hornblende remnant (center) with other terminated remnants of the same crystal, separated from one another by weathering products marking loci of fractures, and from the products by peripheral voids. Both images in cross-polarized light; each field of view is 600 μm wide.

finer than the electron microscope's excitation volume for the EDS signal. Stoichiometries and molar volumes of these or closely related minerals are used in the volumetric calculations of replacement volumes and elemental mobility.

Results of the molar volume calculations are shown in table 2. In the absence of a published molar volume for halloysite, the molar volume of kaolinite (Smyth and Bish, 1988) is used to represent the 1:1 kaolin-group clay product indicated by EDS and XRD. For each element assumed to be immobile, one stoichiometric extremum selected from Helms and others (1987) as discussed in the Methods section produces product/reactant volume ratios closest to isovolumetric, and the other produces the most extreme deviation from isovolumetric replacement for that reactant-product pair.

DISCUSSION

There are two grain-scale mechanisms by which primary silicate minerals in general, and chain-silicates in particular, weather to secondary minerals; transformation and neoformation (Duchaufour, 1982; Eslinger and Pevear, 1988; Nahon, 1991). In *transformation,* the bonds linking the apical oxygens of the silica tetrahedra in the chains of the chain-silicates are locally broken and remade, allowing single- and

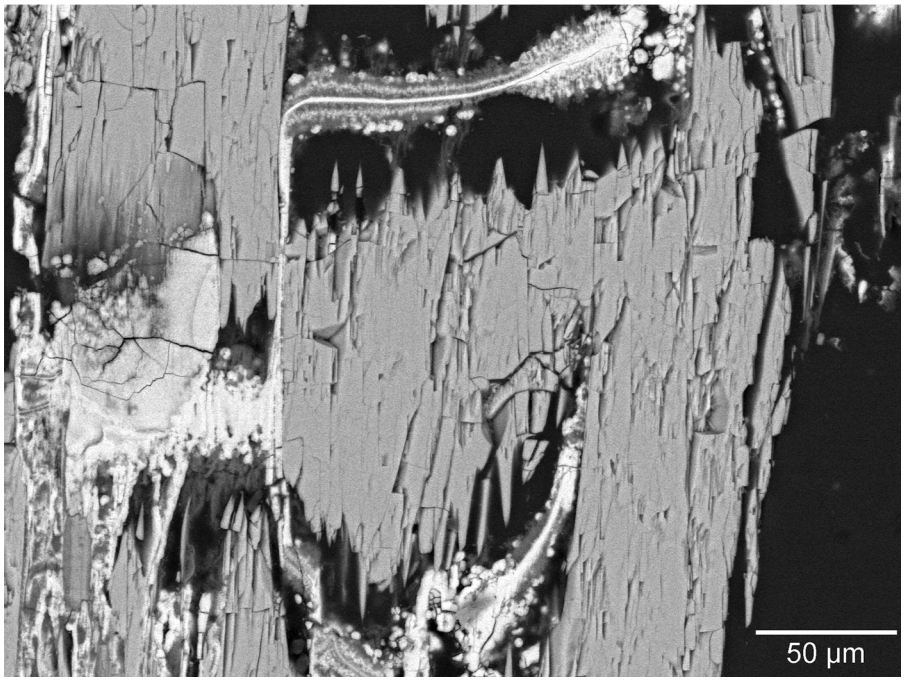

Fig. 4. Doubly terminated denticulated hornblende remnant separated from boxwork consisting of ferruginous and clay-mineral weathering products by a peripheral void. Backscattered electron image.

double-width chains to rearrange and reattach themselves laterally into extensive tetrahedral-octahedral-tetrahedral (T-O-T) sheets, the basic structural unit of 2:1 clays minerals (Eggleton, 1986). Products of transformation reactions are often pseudomorphic (Nahon, 1991) or, in the case of anhedral primary minerals, alteromorphic (in the terminology of Delvigne, 1998) after the primary reactant mineral. In *neoformation,* destruction of primary-mineral bonding is more complete, and secondary minerals are formed, often at some distance from the site of primary-mineral destruction, by crystal-growth of secondary minerals from solutes. Because secondary-mineral formation by precipitation does not require any specific structural relationship with the primary reactant-mineral surface, there is no necessary optical or crystallographic-orientation relationship between primary (reactant) minerals and their neoformation products (Velbel, 1989). These two different mechanisms have different consequences for textural and compositional aspects of reactant-product relationships.

Weathering of Hornblende to Products: Interpretation of Textures

Hornblende corrosion textures.—The earliest weathering stage in this material from the Tallulah Falls Formation (fig. 2) is defined by the corrosion of hornblende and its concomitant replacement by weathering products. These reactions begin at crystal termini and internal surfaces adjacent to grain-traversing fractures and form denticulated terminations as is common in weathered chain-silicates in general (Berner and others, 1980; Berner and Schott, 1982; Delvigne, 1983, 1998; Velbel, 1989, 2007). Denticulation results from side-by-side coalescence of elongate etch pits formed by the anisotropic corrosion of a compositionally and structurally homogenous parent hornblende, with preferential dissolution parallel to the crystallographic *z* axis (Berner and others, 1980; Berner and Schott, 1982; Velbel, 2007). In these early weathering stages,

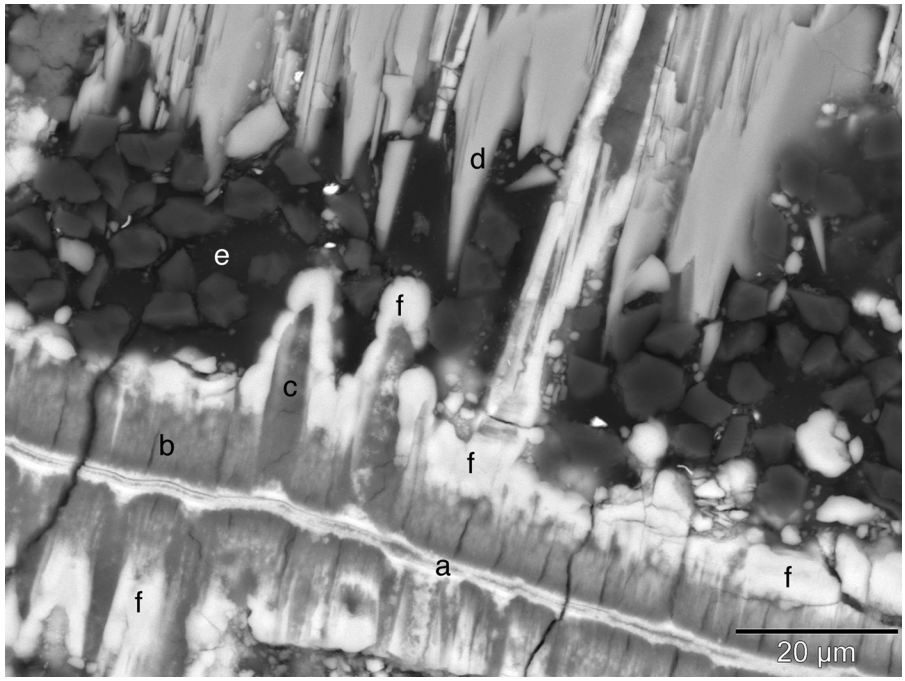

Fig. 5. Ferruginous (high Z-contrast) product (a) marks locus of original fracture transecting hornblende crystal. Lower Z-contrast product (b) formed symmetrically by replacement of hornblende on either side of the fracture, leaving the first-formed (high Z-contrast) product (a) as a "central" parting (common in both serpentinization and weathering of chain-silicates; Velbel, 1989). The replacement front at more advanced stages mimicked the denticulated topography of the remnant hornblende termination, as shown by the two "pendants" (interior of one example is marked (c); (terminology of Velbel, 1989) immediately left of center; note how both project into recesses (etch pits) between denticles. Further corrosion of hornblende formed a typical denticulated termination [(d) Velbel, 1989, 2007], separated from the earlier-formed product by a peripheral void [(e) Velbel, 1989, 2007; Proust and others, 2006]. Note that partings in the low Z-contrast (1:1 clay-mineral) product (b) are parallel to one another and to the denticles of the corroded parent-mineral remnant (d). The high Z-contrast product superposed upon the low Z-contrast product (f) likely formed by precipitation of Fe liberated by continued hornblende dissolution onto the previously formed product (as discussed by Velbel, 1989). The low Z-contrast granular material in the peripheral void is diamond abrasive grit from the thin-sectioning process; such artificially introduced material is absent from most parts of the thin-section (figs. 2-4). Backscattered electron image.

the replacement front is deeply denticulated (etched) with ~10 to 20 μm-scale denticles (fig. 2). Denticles are somewhat larger (~20μm) at more advanced stage of weathering (figs. 3-5) than at earlier stages (fig. 2).

Weathering products.—The relict mafic-ultramafic parent minerals (hornblende, anthophyllite, talc), weathering-produced phyllosilicates [1:1 dioctahedral (aluminous) clay minerals of the kaolin-halloysite group], and weathering-produced hydroxides (goethite, gibbsite) identified by XRD in this study are typical of common minerals in soils developed on weathered metamorphosed mafic and ultramafic rocks throughout the southern Appalachian Blue Ridge and Piedmont, in bulk soils (Rolfe, 1953; Plaster and Sherwood, 1971; Dixon, 1978; Rice and others, 1985; Ogg and Smith, 1993; Schroeder and others, 2000) and specifically in the septo-alteromorphic weathering products of hornblende described by Velbel (1989). Previous clay-mineral studies did not determine whether the specific 1:1 dioctahedral clay mineral present is kaolinite or halloysite. As shown below the specific identity of the 1:1 clay-mineral product of weathering influences the range but not the sign (import or export) of

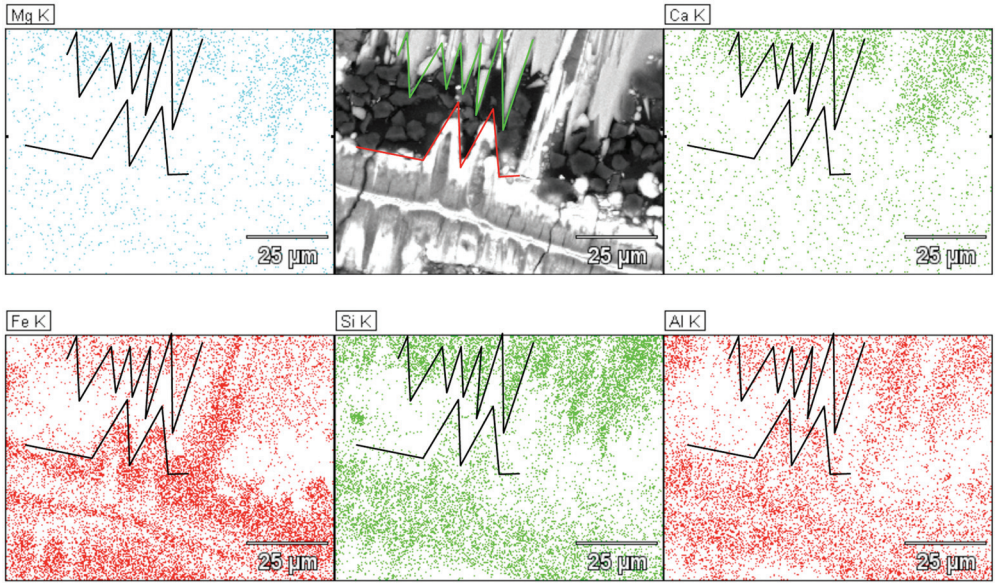

Fig. 6. Elemental maps of Si, Al and Fe, for field-of-view corresponding to figure 5. Note that high Z-contrast features in backscattered electron image (central parting, product lining peripheral void) are Fe-rich, and that low Z-contrast product is richer in Si and Al.

element mobility during early weathering. To be consistent with other recent work in the region (Schroeder and others, 2000), clay-size minerals characterized by 0.706 to 0.736 nm (001) XRD peaks are referred to here as kaolin-group minerals.

Figure 8B shows that most analyzed products are mixtures with widely varying proportions of two phases. One product has a 1:1 Al:Si stoichiometry. The other is dominated by Fe and is interpreted as either goethite with possible Al-for-Fe substitution of up to 20 percent Al or a goethite-dominated mixture with small amounts of gibbsite. Combined with the EDS mapping (fig. 6) showing abundant Si and Al associated with the low Z-contrast material, and XRD of the fine fraction, this suggests that the low Z-contrast material is a kaolin-group mineral, and that the high Z-contrast material is goethite.

Hornblendes in both the Carroll Knob Complex (Velbel, 1989) and the Tallulah Falls Formation exhibit similar weathering and corrosion features and basic mineral relations. The weathering features and products are dominantly septo-alteromorphs (*sensu* Delvigne, 1998; microboxworks) consisting of kaolin-group minerals. Goethite is the ferruginous product at both locations. However, the BEI and EDS data show more internal detail of this ferruginous boxwork than was shown by the previous work of Velbel (1989) on products from the nearby Carroll Knob Complex. For example, in SEI of similar septo-alteromorphs (microboxworks) in the Carroll Knob Complex, a central parting is evident in the morphology of the septa, and pendants project into peripheral voids (figs. 5, 6, and 8 in Velbel, 1989). XRD data for bulk boxwork material from the Carroll Knob Complex show the presence of a kaolin-group clay and goethite (fig. 10 in Velbel, 1989), but the internal distribution and paragenetic sequence of the products (goethite along central parting, kaolin-group clay dominating septa and interiors of pendants, late-stage goethite superposed upon clay-dominated septa and clay-cored pendants) is only apparent in backscattered images and EDS maps of polished thin sections (figs. 5 and 6).

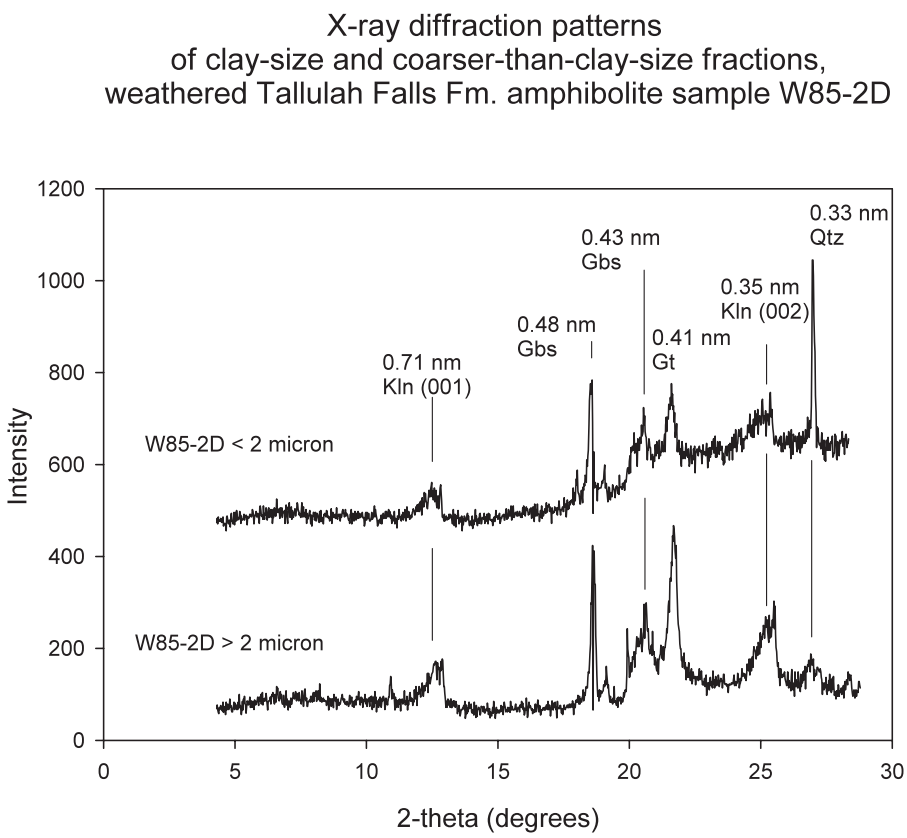

Fig. 7. X-ray diffraction patterns for coarse (below) and fine (above) fractions from the outer weathered portion of the sample examined for this study. The upper trace is offset from the lower by adding 400 counts per channel to the upper pattern. Minerals identified in these patterns are indicated by the d-spacing of the marked peak and the mineral abbreviation (using the standard abbreviations of Kretz, 1983); for the kaolin-group minerals, the Miller indices of the basal and higher-order diffractions are indicated.

Reactant-product relations and petrographic evidence for element mobility, early weathering.— Chain-silicates weather to various products in different environments, requiring different patterns of major-element mobility and immobility. While previous work has examined textures and elemental mobility in early stages of bisiallitic weathering and advanced stages of monosiallitic weathering, previous examinations of early stages of monosiallitic weathering are lacking. The consequences of the present study for elemental mobility are explored in detail below.

The earliest stage of hornblende weathering preserved in the sample examined here is alteration along a fracture transecting the hornblende. The ferruginous (high Z-contrast) product along the central parting (fig. 2) marks the locus of the original fracture transecting the hornblende crystal, along which aqueous solution entered the hornblende and initiated weathering. Subsequently, hornblende corrosion and replacement by a kaolin-group clay product proceeded symmetrically from the fracture, leaving the first-formed (high Z-contrast) product as a central parting, a feature common in both serpentinization and weathering of chain-silicates (Velbel, 1989).

Partings in the low Z-contrast (kaolin-group clay-mineral) product parallel to one another and to the denticles of the corroded parent-mineral remnant (fig. 6) are

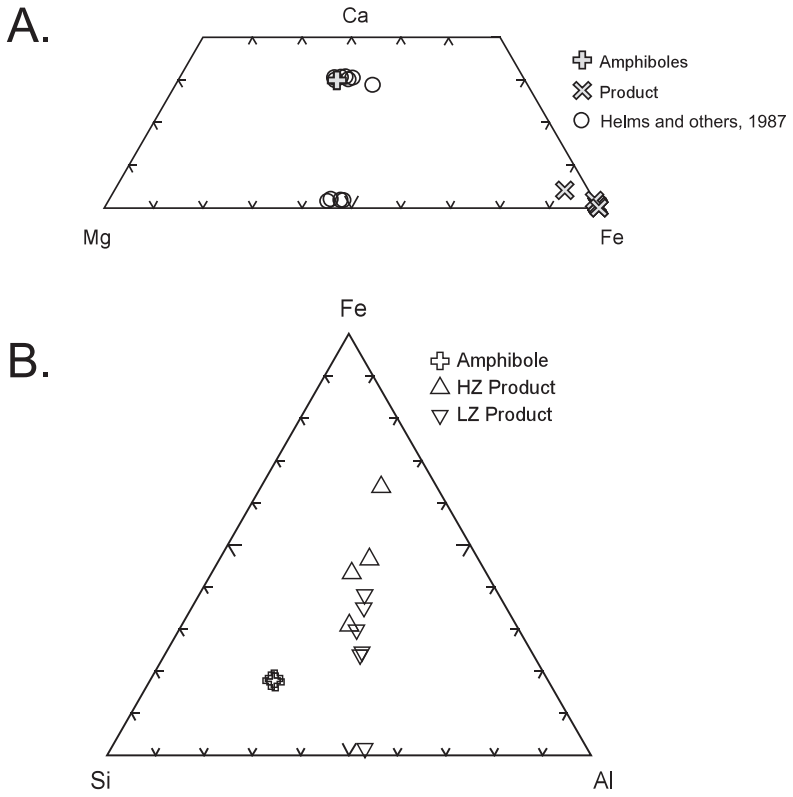

Fig. 8. (A) Lower portion of Mg-Fe-Ca ternary diagram and (B) Al-Fe-Si ternary diagram of EDS point analyses. (A) shows that (1) the Tallulah Falls Formation hornblendes examined in this study are compositionally indistinguishable from the Ca-amphiboles in the adjacent Laurel Creek Complex reported by Helms and others (1987), and (2) the weathering products of Tallulah Falls Formation hornblende examined in this study are very poor in Ca and Mg. (B) shows that most analyzed product has 1:1 Al:Si, and highly variable Fe. Combined with the EDS mapping (fig. 6) and XRD (fig. 7), this suggests that the low Z-contrast material (LZ product) is kaolinite or a related kaolin-group mineral, and that the high Z-contrast material (HZ product) is an iron (oxyhydr)oxide.

consistent with, but do not prove, a topotactic relationship between the layers of the product clay-mineral with chains of the parent mineral during the early-stage weathering and partial replacement. Uniform optical crystallographic orientation within the septa and pendants of ferruginous monosiallitic clay-bearing products after hornblende was reported by Velbel (1989), who suggested (among several possibilities) that the birefringent product material was initially in some form of crystallographic continuity with and transformed from the parent chain-silicate. The petrography of common hornblende weathering textures illustrated here (figs. 2-5) resembles lower-magnification views (Velbel, 1989; photomicrographs 096-101, 138, 312, 313, 375, 376 in Delvigne, 1998).

The isovolumetric character of pseudomorphism or alteromorphism involving complete replacement of a primary mineral by a secondary mineral is often apparent in individual petrographic images (photomicrographs 292, 293, 394, 395 in Delvigne, 1998). The examples cited here (all from Delvigne, 1998) are of naturally weathered chain-silicate minerals, although the same replacement relationships apply to many other weathered silicate minerals as well. Septo-alteromorphs form by a sequence of processes resulting in more complex textures than simple pseudomorphism. The

sequence of stages that results in septo-alteromorphic texture begins with early partial replacement, followed by partial removal without replacement of remaining primary mineral, and ends with complete removal of the last primary-mineral remnants. Early replacement along grain boundaries (photomicrographs 068, 069 in Delvigne, 1998), mineral-crossing fractures (photomicrographs 061, 062, 064, 065, 098, 099, 132, 133 in Delvigne, 1998), or both (photomicrographs 096, 097, 100, 101, 394, 395, 400, 401 in Delvigne, 1998) forms the material that will eventually remain alone as septa. Weathering textures at this early-replacement stage resemble meshwork textures common in partially serpentinized ultramafic rocks (Wicks and Whittaker, 1977). The early partial-replacement stage is followed by partial removal of the remaining primary mineral; at the partial removal stage, each primary mineral remnant is surrounded by a peripheral void (photomicrographs 100, 101, 138, 141, 142, 312, 313, 375, 376 in Delvigne, 1998). Eventually, after complete removal of the remaining primary minerals, only voids remain between the septa of a true septo-alteromorph (microboxwork) (photomicrographs 315-321, 325, 377-380, 444, 445 in Delvigne, 1998).

The isovolumetric character of early replacement in weathered assemblages that eventually appear as septo-alteromorphs is seldom evident from individual images although fortunate combinations of preservation and sampling have produced some examples (photomicrographs 394, 395, 400, 401 in Delvigne, 1998). However, early isovolumetric replacement along grain boundaries and fractures is often evident along with obvious preservation of parent-mineral grain outlines and volume relations with respect to adjacent minerals in petrographic images of samples whose weathering ended at the early stage (photomicrographs 061, 062, 064, 065, 394, 395, 400, 401 in Delvigne, 1998). Similarly, the preservation of texture (and volume) of such early-stage products is indicated in images of samples that weathered beyond the early stage (photomicrographs 141, 142, 377-380, 444, 445 in Delvigne, 1998). By virtue of similarity with the published observations, the internal textures of septa preserved in the sample examined here are interpreted as preserving an early stage of isovolumetric partial replacement like that more completely illustrated by Delvigne (1998).

Among previously published case studies of weathering of individual amphiboles and pyroxenes (see review by Velbel, 2007), a number report simultaneous natural weathering of a reactant chain-silicate and the formation of its weathering products (Eggleton and Boland, 1982; Nahon and Colin, 1982; Proust, 1982, 1985; Delvigne, 1983, 1990, 1998; Colin, ms, 1984; Colin and others, 1985, 1990; Velbel, 1989; Banfield and Barker, 1994; Proust and others, 2006; Velbel and Barker, 2008), and most of these examine chain-silicate weathering in Si-rich smectite forming (bisiallitic) weathering environments. Previous studies of natural weathering of chain-silicates to 2:1 clays suggest, based on structural inferences (Eggleton, 1975; Cole and Lancucki, 1976) and TEM observations (Eggleton and Boland, 1982; Eggleton, 1986; Banfield and Barker, 1994) that (1) the silicate tetrahedra of the primary mineral become the silicate tetrahedra of the alteration product without significant compositional change, and (2) the *x*-axis repeat spacing of I-beams in chain-silicates controls the *z*-axis repeat distance between successive sheets in the 2:1 phyllosilicates that replace chain-silicates. The preliminary inferences of Velbel (1989) and the additional information about internal product textures reported here suggest that similar crystallographic and structural relationships may persist in early-stage products of chain-silicate weathering in monosiallitic weathering environments as well.

Under conditions favoring bisiallitic weathering, Velbel and Barker (2008) observed that smectite can replace pyroxene isovolumetrically if Si is largely or completely immobile. This is more generally the case if tetrahedral units of a parent chain-silicate mineral are inherited directly by the 2:1 phyllosilicate product (Eggleton, 1975; Cole and Lancucki, 1976; Eggleton and Boland, 1982; Eggleton, 1986; Banfield

and Barker, 1994). In contrast, under conditions favoring monosiallitic/allitic weathering, Velbel (1989) observed that Si was mobilized and Al and Fe were immobile during advanced stages of hornblende dissolution and formation of kaolinite, gibbsite, and goethite by precipitation from pore fluids.

The clay-mineral/hornblende replacement front mimics the denticulated topography of the remnant hornblende termination at this early stage of hornblende replacement by clay minerals (fig. 2). However, little or no porosity is observed at the replacement front (fig. 2); early-stage replacement of hornblende by kaolin-group clay-mineral products may be isovolumetric. The denticulated interface of the hornblende (fig. 2) is consistent with an interface-limited dissolution mechanism (Berner, 1978; Berner and others, 1980; Berner and Schott, 1982; Velbel, 1989, 1993a), and inconsistent with a diffusion-inhibiting role for the weathering products (Velbel, 1993a, 2004). Microporosity within the products but too small to observe using conventional SEM may create local surface-chemical microenvironments influencing local solution composition and the kinetics of the fundamentally interface-limited hornblende dissolution reaction (Velbel and Barker, 2008).

Reactant-product relations and petrographic evidence for element mobility, advanced weathering.—At an advanced stage of hornblende weathering to kaolin-group clays and goethite (figs. 4, 5), early-formed ferruginous (high Z-contrast) product persists and continues to mark the central parting, the locus of a fracture transecting the original hornblende crystal (figs. 4-6). Kaolin-group material is symmetrically distributed on either side of the central parting, apparently preserved as formed during earlier stages of weathering (fig. 2).

The clay-mineral/hornblende replacement front that mimics the denticulated topography of the remnant hornblende termination at early stages of hornblende replacement by clay minerals (fig. 2) is preserved at more advanced stages as shown by the two "pendants" (terminology of Velbel, 1989) immediately left of center in figure 5; note how both project into etch pits between denticles. Further corrosion of hornblende beyond the temporary early isovolumetric-replacement (septum-forming) stage formed a typical denticulated termination (figs. 3-6; Velbel, 1989, 2007), separated from the earlier-formed product by a large, continuous peripheral void (figs. 3-6; Velbel, 1989, 2007; Proust and others, 2006). As previously inferred by Velbel (1989), the peripheral void implies that at this intermediate stage the weathering products no longer form by volume-for-volume replacement as was the case during the early stage of the reaction, but instead large volumes of hornblende are dissolved stoichiometrically (reaction 1 of Velbel, 1989) and smaller volumes of secondary minerals form by precipitation from solutes (reactions 2-4 of Velbel, 1989). Velbel (1989) suggested that pendants were late-stage precipitates (neoformed), but the internal textural relations observed in this study (figs. 5, 6) suggest that the clay-mineral cores of the pendants are preserved projections into earlier smaller etch pits between denticles (as in fig. 2), and that only the surface coating of high Z-contrast Fe-rich material is neoformed as previously suggested. The goethite (high Z-contrast) superposed upon the kaolin-group clay mineral likely formed as continued hornblende dissolution liberated Fe which subsequently precipitated onto the previously formed product, similar to the ferruginous boxwork structures of the Carroll Knob Complex (Velbel, 1989). Even during the precipitation of late-stage ferruginous products and continued dissolution of hornblende, there is little or no volume change in the earlier-formed secondary product (figs. 4, 5).

Elemental Mobility and Reactant-Product Volume Relationships

In this section, we quantify limits on the mobility of Si and Al required to be consistent with the observed mineral compositions, textures, and structures in the weathered Tallulah Falls Formation. We compare the inferred implications for Si and

Al mobility of our mineral-scale results with (1) similar inferences from previously published work on tropical and humid temperate weathering, particularly of ultramafic rocks, (2) whole-rock geochemical/groundwater composition comparisons in deeply weathered mafic parent materials in humid temperate landscapes, (3) long-term Si and Al mobilization inferred from saprolite and soil solid-phase bulk chemistry elsewhere in the region (Georgia Blue Appalachian Ridge and South Carolina Appalachian Piedmont), and (4) whole-rock geochemical/surface water composition comparisons in deeply weathered humid temperate and tropical landscapes.

Implications of early-stage mineral relations for sources for Si and Al.—Alkaline earths (Mg, Ca) were detected by EDS in parent minerals (figs. 6, 8A); complete loss of alkaline earths during product formation is indicated by the absence of these elements from EDS maps of the products (fig. 6) and EDS spot analyses (fig. 8A). A simplified balanced chemical reaction invoking the conventional assumption that Al is immobile can be written for the weathering of tschermakite (as a simplified representation of hornblende) to any kaolin-group mineral as the silicate-bearing weathering product and goethite as the Fe-bearing weathering product:

$$2Ca_2(Mg_3AlFe^{+3})(Si_6Al_2)O_{22}(OH)_2 + (7 + 3n)H_2O + 20H^+ \rightarrow$$
$$3Al_2Si_2O_5(OH)_4 \cdot nH_2O + 2FeO(OH) + 6H_4SiO_4 + 4Ca^{2+} + 6Mg^{2+} \quad (2)$$

where $n = 0$ for kaolinite, dickite, nacrite, or dehydrated ("7-Å") halloysite, and $n = 2$ for hydrated ("10-Å") halloysite (once more commonly known as endellite; Pundsack, 1956). In this simplified, conventionally written (Al-immobile) reaction, three moles of kaolin-group mineral and two moles of goethite form from the weathering of two moles of hornblende. Using the molar volumes of pargasite (for hornblende, in the absence of a published molar volume for hornblende or tschermakite), kaolinite (for the least-hydrated possible kaolin-group mineral) and goethite from Smyth and Bish (1988) summarized in table 2, two moles of parent amphibole ($2 \times 274.94 = 549.88$ cm^3) produce three moles of kaolinite ($3 \times 99.236 = 297.708$ cm^3) and two moles of goethite ($2 \times 20.693 = 41.386$ cm^3) for a total product volume of 339.094 cm^3. In other words, if a product assemblage of kaolinite plus goethite formed from hornblende without import or export of Al, one volume of hornblende would be replaced by $339.094/549.88 = 61.67$ volume percent of the product-mineral assemblage. However, the texture of the kaolin-group weathering product that replaced hornblende symmetrically (beginning from the central parting) during early hornblende weathering (figs. 2, 3B, 4, 5, 6) lacks discernable porosity (fig. 2 and esp. fig. 5). Therefore, at early stages of hornblende weathering, either the silicate product that formed had a larger molar volume than kaolinite, or Al was imported into the hornblende early-weathering environment to form a greater (mass and volumetric) abundance of lower-molar-volume product than the amounts that would result from the assumption of immobile Al behavior (reaction 2). The next paragraphs explore these alternatives.

Unit-cell parameters sufficient to determine the molar volume of halloysite do not exist for any of halloysite's common hydration states. However, since kaolinite and halloysite have the same Al:Si stoichiometry, differences in bulk densities are attributable to differences in the volume of the 1:1 layer-silicate structure and not to differences in cation composition of the mineral. The bulk density of kaolinite is 2.601 g/cm^3 for the structure from which the molar volume used in this paper was determined (Smyth and Bish, 1988). The bulk density of dehydrated halloysite is nearly identical, 2.56 g/cm^3 (Pundsack, 1956). However, the bulk density of hydrated ("10-Å") halloysite is 2.10 g/cm^3 (Pundsack, 1956). Consequently, a unit volume of kaolinite and a volume of hydrated halloysite $2.56/2.10 = 1.22$ times the unit volume would contain the same quantity of Al and Si.

Referring to the data in the last two columns of table 2 we can compare the molar volumes for reactant-product pairs. High-quality molar volume data are available for kaolinite, so kaolinite is used as the silicate product in these volume estimates. As shown in the previous paragraph, if hydrated halloysite is the actual product mineral, the volume of halloysite produced will be 22 percent greater than (or 1.22 times) the values shown in the last two cells of the Si-immobile and Al-immobile rows of table 2. Thus, if the product actually present is halloysite and Si is immobile, $1.38 < V_{halloysite}/V_{hornblende} < 1.50$. In other words, regardless of whether the product is kaolinite ($1.13 < V_{kaolinite}/V_{hornblende} < 1.23$; table 2, Si-immobile row) or halloysite ($1.38 < V_{halloysite}/V_{hornblende} < 1.50$; 1.22 times the last two values in table 2, Si-immobile row), the volume of product formed will exceed the volume of hornblende replaced if Si is immobile, and some of the Si could be removed and still leave enough Si for isovolumetric early-stage replacement ($V_p/V_r = 1$) of hornblende by either kaolinite or halloysite.

Similarly, but more significantly, if the product actually present is halloysite and Al is immobile, $0.440 < V_{halloysite}/V_{hornblende} < 0.617$ (1.22 times the last two values in table 2, Al-immobile row). In other words, regardless of whether the product is kaolinite ($0.361 < V_{kaolinite}/V_{hornblende} < 0.506$; table 2, Al-immobile row) or halloysite ($0.440 < V_{halloysite}/V_{hornblende} < 0.617$, 1.22 times the last two values in table 2, Al-immobile row), the volume of kaolin-group product formed cannot exceed 62 percent ($V_p/V_r < 0.62$) of the volume of hornblende replaced if Al is immobile; accounting for the maximum volume of goethite formed assuming immobility of Fe in oxidized weathering environment raises the volume percent of both products to a maximum value of 74 percent ($V_p/V_r < 0.74$). The volume of monosiallitic products formed from the Al and Fe in a unit volume of hornblende would have a void fraction of at least 26 percent. In order to form the non-porous ($V_p/V_r = 1$) early-stage product observed, Al must have been imported into the early-stage hornblende-product replacement microenvironment, regardless of whether the silicate product is kaolinite or halloysite.

For early-stage replacement of hornblende by a kaolin-group mineral to be isovolumetric (as implied by the petrography of the Fe-poor product mineral in figs. 2, 5 and 6), a new reaction from hornblende to products can be written, retaining volume rather than Al. The product with the largest molar volume (most volume per Al) requires the least import of Al, so the volumetric relationships of table 2 are again adjusted for the lowest-density (fully hydrated) variety of halloysite. In other words, $(2.56/2.10) \times 99.236\ cm^3/mole_{kaolinite} = 121\ cm^3/mole_{hydrated\ halloysite}$. For isovolumetric replacement ($V_p/V_r = 1$) and accounting for the volume of the one mole of goethite formed if the one mole of Fe per mole of hornblende is immobile, one mole of hornblende (274.94 cm^3/mole) is replaced by (274.94 − 20.693 =) 254.247 cm^3 or (254.247/121 =) 2.10 moles of fully hydrated halloysite. Thus, accounting for the small volume of goethite formed, ignoring details of Al speciation, and using the same simplified hornblende formula as above, the balanced reaction for (early-stage) *isovolumetric* replacement of hornblende by *hydrated halloysite* would be

$$Ca_2(Mg_3AlFe^{+3})(Si_6Al_2)O_{22}(OH)_2 + 8.3H_2O + 6.4H^+ + 1.2Al^{3+} \rightarrow$$
$$2.10Al_2Si_2O_5(OH)_4 \cdot 2H_2O + FeO(OH) + 1.8H_4SiO_4 + 2Ca^{2+} + 3Mg^{2+} \quad (3)$$

Reaction (3) is volume-balanced assuming formation of the fully hydrated halloysite, the kaolin-group product with the largest possible molar volume. If the product is a lower molar-volume kaolin-group mineral (for example, kaolinite or dehydrated halloysite), and accounting for the volume of the one mole of goethite formed if the one mole of Fe per mole of hornblende is immobile, one mole of hornblende (274.94 cm^3/mole) is replaced by (274.94 − 20.693 =) 254.247 cm^3 or (254.247/99.236 =) 2.56 moles of kaolinite. Again accounting for the small volume of goethite formed,

ignoring details of Al speciation, and using the same simplified hornblende formula as above, the balanced reaction for (early-stage) *isovolumetric* replacement of hornblende by *kaolinite* would be

$$Ca_2(Mg_3AlFe^{+3})(Si_6Al_2)O_{22}(OH)_2 + 4.56H_2O + 3.64H^+ + 2.12Al^{3+} \rightarrow$$
$$2.56Al_2Si_2O_5(OH)_4 + FeO(OH) + 0.88H_4SiO_4 + 2Ca^{2+} + 3Mg^{2+} \quad (4)$$

All major elements except Al behave similarly whether hornblende weathers to a kaolin-group mineral with Al immobile (reaction 2), or is initially isovolumetrically replaced at septa by halloysite (reaction 3) or by kaolinite (reaction 4). Overall, water and environmental acidity are consumed, and Ca, Mg, and some Si, are released into solution. In reaction (2) Al is assumed to remain in the solid products. However, as noted above, there is not enough Al present in the replaced volume of reactant hornblende to produce the observed initial isovolumetric replacement at septa. In contrast, reactions balanced in accordance with the observation of early-stage isovolumetric replacement (reactions 3 and 4) require only commonly observed behavior of most major elements, but also highlight the fact that the preserved early-stage textural distribution of product requires that Al was mobile and must have been imported into the early replacement microenvironment. Furthermore, this holds regardless of whether the weathering product is kaolinite or halloysite; the only differences between reactions 2 through 4 are in the amounts of Al imported into and Si exported from the replacement microenvironment. Reaction (4) requires the import of more Al into the early-stage isovolumetric partial alteromorph of kaolinite after hornblende than is required to form a similar halloysite alteromorph (reaction 3). Thus, reaction (3) defines the lower limit, and reaction (4) the upper limit, of Al import required for isovolumetric early-stage weathering and replacement of hornblende.

For the Tallulah Falls Formation hornblende, replacement by a dehydrated kaolin-group mineral is essentially isovolumetric ($V_p/V_r = 1.0$) if Si is immobile ($V_p/V_r = 1.13$, table 2). This is consistent with the widely accepted mechanism by which tetrahedral chains in pyroxene and amphibole are rearranged into the tetrahedral sheets of layer-structured weathering products (for example, Eggleton, 1975 for pyroxene; Cole and Lancucki, 1976 for amphibole), resulting in volume-for-volume replacement and pseudomorphism of chain-silicates by phyllosilicates. This phenomenon has been observed at unit-cell scales by transmission electron microscopy (TEM) for alteration of chain-silicates to 2:1 phyllosilicates during aqueous alteration; examples include pyroxene altering to talc (Eggleton and Boland, 1982) and amphibole weathering to smectite (Banfield and Barker, 1994). This suggests that weathering of hornblende to kaolin-group minerals in northern Georgia is consistent with mechanisms of chain-silicate weathering elsewhere, and with the assumption of overall isovolumetric weathering assumed in the elemental-mobility calculations of Gardner (1992).

Co-occurring primary minerals as potential sources for Si and Al.—As noted above, Tallulah Falls Formation hornblende does not contain enough Al for early-stage isovolumetric replacement by an Al-bearing clay-mineral. If the volume of observed kaolin-group product is equal to the volume of hornblende destroyed (reactions 3 and 4 above), the abundance of the Al present in the hornblende would be sufficient to form no more than 62 percent of the volume of clay-mineral product, ultimately requiring flux of Al from an external source to satisfy this mass balance (table 2 and discussion above). Different amounts of Al would be required to form products with similar cation stoichiometry but different molar volumes (for example, halloysite, reaction 3 and kaolinite, reaction 4), but Al import is still required regardless of the specific identity of the kaolin-group clay mineral that forms as the weathering product.

Possible sources for such Al external to the local parent hornblende and its pseudomorphic/alteromorphic products include local Al-silicates that weather as rapidly as or faster than hornblende, and Al transported from elsewhere in the regolith-soil-landscape system. Both phenomena have been previously reported from studies of natural tropical deep-weathering products of crystalline rock. For example, Nahon and others (1982) reported the formation of smectite with up to 2.170 Al per $O_{20}(OH)_4$ smectite formula unit occurring as pseudomorphs after forsterite with only 0.013 Al per O_4 olivine formula unit in ultramafic rocks (partially serpentinized dunite) weathered under humid tropical conditions of the Ivory Coast. Al needs to be mobile in order to form Al-bearing smectite from Al-poor olivine; Nahon and others (1982) invoke simultaneous dissolution of adjacent Al-bearing enstatite as the source of the Al in the smectite pseudomorphic after olivine. Similarly, Colin and others (1985, 1990) reported the formation of smectite with an average of 0.782 Al per $O_{10}(OH)_2$ smectite formula unit occurring as alteration products of enstatite and diopside with only 0.054 and 0.068 Al, respectively, per O_6 pyroxene formula unit in ultramafic rocks (pyroxenite) weathered under humid tropical conditions of Brazil. The abundance of Al in the smectite associated with weathered but Al-poor pyroxenes (Colin and others, 1985, 1990) suggests that Al needs to be mobile in order to form the observed Al-bearing smectite from Al-poor pyroxenes.

Amphibolites in the region of this study contain plagioclase feldspar (for example, Helms and others, 1987; Velbel, 1992). In the southern Blue Ridge Mountains, hornblende and plagioclase weather at almost exactly the same rate per unit modal abundance (Velbel, 1992). This is consistent with experimentally determined rates (for example, Brantley and Chen, 1995; Blum and Stillings, 1995), and with Goldich's (1938) empirical weathering series. However, plagioclase in the region weathers to kaolin-group minerals, retaining Al (Velbel, 1983, 1985a, 1985b); thus, plagioclase weathering is not a likely external source of Al required for isovolumetric replacement of hornblende by kaolin-group clays.

Other Al-bearing phases common in regional amphibolites include staurolite, kyanite, and garnet (Hatcher, 1976). All three of these minerals have been reported from the adjacent Laurel Creek Complex (Helms and others, 1987); trace quantities of staurolite and small amounts of possible weathering products of garnet occur in the Tallulah Falls Formation sample examined here. Staurolite (Velbel and others, 1996) and kyanite (Velbel, 1999) weather very slowly and therefore are not likely to yield much dissolved Al for export to the weathering products of other minerals. Although a few small "limonite" nodules like those formed by complete pseudomorphic/alteromorphic replacement of garnet (Velbel, 1984) do occur in the Tallulah Falls Formation amphibolite, no unweathered garnet was found in this sample to prove unequivocally the presence of garnet in the sample. However, garnet is widespread in the schists and amphibolites of the Tallulah Falls Formation (Hatcher, 1976), and constitutes up to 10 percent modal percent of structurally juxtaposed Laurel Creek Complex amphibolite units (McSween and Hatcher, 1985; Helms and others, 1987). Furthermore, garnet weathers rapidly enough to contribute significant solutes to regional soil- and surface-water (Velbel, 1985a; Taylor and Velbel, 1991; Price and others, 2005). Garnet does not form weathering products in soil where Al and Fe are observed to have been completely removed from etched garnet surfaces, preventing the local incorporation of Al and Fe into weathering products (Velbel, 1984, 1993a; Velbel and others, 2007). In these environments, Al and Fe released by garnet weathering in soils are available to be transported as solutes elsewhere and incorporated into the weathering products of other minerals distant from the dissolving soil garnets. Furthermore, although gibbsite and goethite form from garnet in saprolite (Velbel, 1984), garnet contains Fe and Al in excess of the amounts required for

isovolumetric replacement of garnet by Fe and Al (oxy)hydroxide weathering products (Velbel, 1993a). Up to 10 to 15 percent of the Al and Fe produced during garnet weathering could be removed from the garnet-weathering microenvironment, leaving enough residual Al and Fe to form the observed gibbsite-goethite pseudomorphs/alteromorphs (Velbel, 1993a). Aluminum derived from weathered garnet in southern Blue Ridge amphibolites and adjacent structurally juxtaposed metasedimentary units might contribute to the Al required for Si-immobile isovolumetric replacement of hornblende by kaolin-group minerals during the early stages of hornblende weathering (reactions 3 and 4).

Garnet weathering may contribute to the Al that would be required to isovolumetrically replace hornblende with 1:1 clay if Si is immobile or minimally mobile during early clay formation. In the absence of garnet weathering or some other Al source, direct isovolumetric weathering of hornblende to 1:1 clay mineral is not possible in this study area; instead, Al immobility, loss of dissolved Si, and formation of appreciable porosity is implied (table 2). In this case, perhaps there is high porosity in the weathering product that is too small to be resolved by conventional SEM (Velbel and Barker, 2008). Another possibility is that a no-longer-preserved intermediate stage of chain-silicate weathering isovolumetrically to smectite as observed by Banfield and Barker (1994) and Velbel and Barker (2008) has been followed by degradation of the earlier-formed smectite to the present kaolin-group clay.

Elemental mobility is simpler and less equivocal at more advanced stages of hornblende weathering. Velbel (1993a) showed that even end-member Fe-rich pyroxenes and amphiboles do not contain enough Fe to produce a volume of product equal to the volume of reactant replaced, and the present results are consistent with the earlier findings. Allowing for substantial Al in the Tallulah Falls amphibole of the present study, molar-volume calculations invoking immobility of Al and Fe (table 2) indicate that Al-Fe-rich products of hornblende weathering should have high porosity. The abundances of boxwork and peripheral voids observed here (figs. 2-6) are qualitatively consistent with the quantitative petrographic measurements of hornblende weathering products in similar weathered materials elsewhere in the vicinity (Velbel, 1989). Furthermore, scenarios involving immobility of Al and Fe allow substantial export of Si while still forming volumes of 1:1 clays consistent with textural observations, and appear reasonable given the known high rainfall and solute dynamics of the region (for example, Velbel, 1992).

Relationship to Si and Al mobility at larger spatial scales.—Direct evidence for extensive Al loss and long-distance transport from other parts of the regolith-soil-landscape system to the hornblende-bearing sample of the present study is presently lacking. However, some preliminary inferences are possible. Several papers have compared Al and Si mobility in saprolite with the dissolved abundances of the same elements in associated pore solutions and surface waters. Gardner (1992) and White and others (1998) examined Al and Si mobility in saprolites of deeply weathered, low-relief landscapes in the Appalachian Piedmont of South Carolina, similar landscapes of Brazil, and high-relief upland saprolitic landscapes of Puerto Rico, with abundances of the same elements in surface waters from the same landscapes. Both Gardner (1992) and White and others (1998) observed that long-term molar ratios of Si to Al leached from regolith solids during weathering are lower than the dissolved Si:Al ratios in regolith pore waters and many times lower than dissolved Si:Al ratios in rivers of these same landscapes (table 3). Thus, time-integrated loss of Al from deep humid-temperate and tropical regoliths is many times greater than can be accounted for by Al fluxes associated with present-day solutes. Gardner (1992, table 2) calculated the dissolved Al abundances expected from saprolite chemistry and dissolved Si concentrations. The most extreme values (lowest Si/Al ratios, highest expected dissolved Al) are

TABLE 3

Molar Si/Al ratios from published studies of deep weathering

Setting	Saprolite			Solutes in	Solutes			Source
	Min.	Average	Max.		Min.	Average	Max.	
South Carolina and Georgia	2.9	5.91	19.4	Streams	60	92.9	128	Gardner (1992)
Brazil	4.46	10.4	34.4	Streams	15.3	115.6	231	Gardner (1992)
E. Puerto Rico	1.78	2.91	3.91	Regolith pore fluids	6.74	15.6	22.6	White and others (1998)
E. Puerto Rico				Streams		>1000		White and others (1998)

from saprolites developed from mafic/ultramafic parent rocks (basalt, 4.82; diabase, 3.60; gabbro, 2.90; amphibolite, 4.80; and amphibolite schist, 4.46; compare the preceding values from Gardner, 1992, table 2, with table 3 in this paper). Gardner (1992) hypothesized pH variation resulting from carbon-dioxide/carbonic acid re-equilibration during soil water emergence in the riparian zone. This process could account for the removal of Al from saprolite without the Al appearing in dissolved form in streams; alternatively, the saprolite Si/Al ratios might be relict and unrelated to present solute abundances (Gardner, 1992). However, neither of these suggestions addresses specifically why mafic-ultramafic materials would be the most influenced among all rock types.

The results of the present study suggest another alternative; that Al is as mobile as the low regolith Si:Al ratios imply (Gardner, 1992), but that the Al is mobilized to greater depths in the weathering profile, to incipiently weathered materials below the sampled saprolite part of most weathering profiles. Such materials, within which silicate-minerals would be as weathered as or even less weathered than the earliest stage of hornblende weathering examined here, could act as sinks for dissolved Al. Such incipiently weathered materials are required for isovolumetric weathering of mafic silicates to clays as observed here. Such large-scale but within-landscape redistribution of Al could account (1) for the Al mobility required by the isovolumetric early replacement observed here, and (2) the absence of dissolved Al levels consistent with the long-term removal of Si and Al from saprolite observed by Gardner (1992) and White and others (1998). Furthermore, saprolite Si:Al ratios decrease almost monotonically down-profile in the Puerto Rican saprolite profile examined by White and others (1998). If Al were immobile, this would imply up-profile enrichment in Si relative to Al. However, the observed vertical distribution of Si:Al ratios could instead result if Al is leached from high in the profile, transported down-profile, and accumulates in the least weathered saprolite just above the bedrock. Down-profile (vertical) and down-slope (lateral) transfer of minimally soluble elements (Al, Fe) as solutes are necessary to account for the observed distribution of Al in tropical bauxitic and lateritic weathering profiles on granitic parent materials in Africa and South America (for example, Boulangé, 1984, 1987; Delvigne, 1998).

The potential relevance of Al mobilization from predominantly felsic rocks to the early weathering of mafic rocks in this study is exemplified by Schroeder and others (2000). Schroeder and others (2000) applied several long-established approaches in a novel way to link observed weathering profile-scale changes and global elemental cycling. Their groundwater/regolith solid-phase study focuses on metamorphosed mafic rocks similar to those in this study. Schroeder and others (2000) compared their data on element-depletion from the profile not with a short-term solute record (as is

common in many previous studies; see reviews by Velbel, 1993b; White, 1995, 2005), but with a long-term solute record, the solute composition of regional groundwater. The bicarbonate/silica release ratio inferred from long-term time-integrated depletion in the preserved part of the residual/erosional upland profile is six times higher than the long-term time-integrated ratio observed in groundwaters in the Appalachian Piedmont of Georgia (U.S.A.). This groundwater chemistry reflects weathering processes that consume little carbonic acid and produce little bicarbonate for the amount of silica produced, consistent with weathering of felsic rock. From these observed differences, Schroeder and others (2000) inferred that the groundwater signature is dominated by more extensive and deeply weathered felsic terrains, rather than the weathering of the meta-gabbro unit they study in detail. Consequently, where mafic-ultramafic rock bodies occur juxtaposed against felsic rock types, over the long term Al may be transferred from products of Al-rich felsic-rock weathering to products of Al-poor mafic-ultramafic-rock weathering like those examined in this study.

Summary.—Isovolumetric replacement of chain-silicates by clays requires immobility of enough Si to form the observed volumes of product in both bisiallitic (Velbel and Barker, 2008) and monosiallitic (this study) weathering regimes. In both cases examined to date, strict immobility of Si would produce greater-than-isovolumetric abundance of clay minerals, allowing that some fraction of Si initially present in the parent mineral may be removed from the replacement microenvironment and still allow isovolumetric replacement. Immobility or minimal mobility of Si resulting in isovolumetric replacement of mafic silicates by clays requires import of other clay-forming elements to the pseudomorph. At early stages of hornblende weathering in the present study, Al is apparently mobile and imported into the hornblende weathering microenvironment. The required Al may be imported from nearby garnet-pseudomorph weathering microenvironments (Velbel, 1984, 1993a; Velbel and others, 2007) where Al is complexed and soluble (Velbel, 1984; White and others, 1998) and/or produced in excess of the amounts required by its own weathering products (Velbel, 1993a). Alternatively, prolonged weathering of felsic rocks may mobilize Al (for example, as required by many observations of bauxitization of felsic rocks; for example, Boulangé, 1984, 1987; Delvigne, 1998) and transported as solutes from the felsic-rock weathering environments to the mafic-rock weathering environments, as implied by the observations and inferences of Schroeder and others (2000). At more advanced stages of weathering, Fe is mobilized from dissolving hornblende, transported in dissolved form across the peripheral void (Velbel, 1989) and precipitated as late-stage goethite on pendants.

Immobility or minimal mobility of Si and mobilization of ostensibly immobile elements (Al, Fe) appears to contradict conventional wisdom. However, this required elemental behavior is not unique to the present study; similar immobility/minimal mobility of Si and import of Fe is required to form smectite pseudomorphs after pyroxene in West Africa (Velbel and Barker, 2008). In both cases, the specific observed compositional and molar-volume relationships favor structurally controlled isovolumetric replacement of chain-silicates by sheet silicates at the earliest stages of weathering. Interestingly, the closest-to-isovolumetric reactant-product pairs in both Velbel and Barker (2008) and this study both involve (1) immobility of silica during the earliest stage of replacement, and (2) formation of the collapsed, least-hydrated states of the product clay minerals. Both phenomena are consistent with the widely inferred transformation mechanism of early-stage chain-silicate weathering by which tetrahedral units of the parent chain-silicate mineral are inherited directly by the (generally 2:1) phyllosilicate product (Eggleton, 1975; Cole and Lancucki, 1976; Eggleton and Boland, 1982; Eggleton, 1986; Banfield and Barker, 1994).

Preferred mobilization of Si over Al or Fe eventually occurs in natural weathering of chain-silicate minerals to clay minerals, but only at more advanced weathering stages than the stage of partial pseudomorphic (septo-alteromorphic) replacement. The earliest stages of chain-silicate weathering appear to involve well-understood reactant-product structural relationships that in turn require different major-element behavior, including immobility of Si and mobilization of Al and/or Fe (Velbel and Barker, 2008, and this study) than is common at more advanced stages of mineral weathering and mineral-water interactions.

The dissolved Al and Fe species that allow these elements to be mobilized over the observed distances may include inorganic species and chelated organic compounds (possibly biologically mediated), but specific aqueous species cannot be determined from this study alone. Further research is required to understand the relationship between mobility of Al and Fe at mineral-reaction scales and whole-sample/-profile/-landscape scales during weathering of mafic-ultramafic rocks, especially (1) research using higher-magnification/higher-resolution imaging and analytical methods; (2) research integrating earlier bisiallitic (smectite-forming) stages of chain-silicate weathering with more advanced monosiallitic stages in the same weathering profiles, and (3) research on mobility/immobility/import/export behavior of the same elements during the simultaneous weathering of possible Al-source minerals (for example, garnet) within the same parent-rock unit, and in adjacent units with which a weathered mafic unit might exchange solutes.

CONCLUSIONS

Hornblende weathering textures formed under thoroughly leached, oxidizing conditions in northeast Georgia (U.S.A.) and imaged in the present study using backscattered electron imaging of polished thin-sections shed new insight into the origins of similar textures and products previously observed using optical petrography and secondary electron imaging. Even at the earliest weathering stage preserved in this material, corrosion of hornblende forms typical denticulated terminations, but little porosity is apparent within the weathering product or between it and the reactant mineral at this stage. More advanced weathering of hornblende forms typical denticulated terminations, separated from the earlier-formed product by a large, continuous peripheral void; porosity is much more conspicuous at this stage. Internal textures and volumetric relationships between naturally weathered hornblende and preserved early-stage weathering products (boxworks and pendants consisting of 1:1 clays) are consistent with (1) either solid-for-solid isovolumetric replacement with Si immobility/minimal mobility and Al mobilization at the mineral scale or replacement of solid parent mineral by product with substantial nano-scale porosity too small to observe with conventional SEM at early stages of hornblende weathering, (2) short-distance transport but smaller-than-grain/pseudomorph-scale retention of Al and Fe during advanced stages of weathering, and (3) leaching of substantial Si and all base cations at advanced stages of weathering. Elemental behavior at the advanced stage of weathering is consistent with the high exported-dissolved Si:Al of present-day solute exports (Velbel, 1985a, 1985b; Gardner, 1992; White and others, 1998). However, the immobile/minimally mobile behavior of Si and import of Al into the weathering products of hornblende required by the molar-volume relationships for isovolumetric early weathering implies larger-scale mobilization of Al. External fluxes of Al and Fe can be from coexisting primary minerals whose weathering can produce excesses of these elements, extensive weathering of neighboring felsic rocks, and/or spatio-temporal variation in Si mobilization with extent of weathering that may be consistent with the results of Gardner (1992), White and others (1998), and Schroeder and others (2000) based on bulk-sample-scale and profile-scale chemical and mineralogical data.

ACKNOWLEDGMENTS

We thank Ewa Danielewicz (Michigan State University Center for Advanced Microscopy) for assistance with the scanning electron microscopy, and Vaneet Aggarwal and Brian Teppen (MSU Department of Crop and Soil Sciences) and Lisa Kelly (MSU Honors College) for assistance with XRD of the fine fractions. We are grateful to Jason R. Price for helpful communications about garnet weathering, and to Tim Drever, Don Rimstidt, and an anonymous reviewer, for their helpful reviews. This research was supported by a grant from the Michigan State University Office of International Studies and Programs, and NASA Grant NNG05GL77G.

References

April, R. A., and Newton, R. M., 1983a, Mineralogy and chemistry of some Adirondack Spodisols: Soil Science, v. 135, p. 301–307, doi:10.1097/00010694-198305000-00005.

——— 1983b, Neutralization of acid deposition in sensitive bedrock terrains: Control of surficial geology on lake acidification, *in* Nahon, D., and Noack, Y., editors, Pétrologie des Altérations et des Sols, Volume III: Sciences Géologiques, Mémoires (Strasbourg), v. 73, p. 19–30.

——— 1985, Influence of geology on lake acidification in the ILWAS watersheds: Water, Air, and Soil Pollution, v. 26, p. 373–386.

April, R. A., Newton, R. M., and Coles, L. T., 1986, Chemical weathering in two Adirondack watersheds: Past and present-day rates: Geological Society of America Bulletin, v. 97, p. 1232–1238, doi:10.1130/0016-7606(1986)97⟨1232:CWITAW⟩2.0.CO;2.

Banfield, J. F., and Barker, W. W., 1994, Direct observation of reactant-product interfaces formed in natural weathering of exsolved, defective amphibole to smectite: Evidence for episodic, isovolumetric reactions involving structural inheritance: Geochimica et Cosmochimica Acta, v. 58, p. 1419–1429, doi:10.1016/0016-7037(94)90546-0.

Becker, G. F., 1895, A reconnaissance of the goldfields of the southern Appalachians: U.S. Geological Survey, 16th Annual Report, Pt. 3, p. 251–331.

Berner, E. K., and Berner, R. A., 1996, Global Environment: Water, Air, and Geochemical Cycles: Upper Saddle River, New Jersey, Prentice Hall, 376 p.

Berner, R. A., 1978, Rate control of mineral dissolution under earth surface conditions: American Journal of Science, v. 278, p. 1235–1252.

——— 2004, The Phanerozoic Carbon Cycle: CO_2 and O_2: New York, Oxford University Press, 150 p.

——— 2006, Inclusion of the weathering of volcanic rocks in the GEOCARBSULF model: American Journal of Science, v. 306, p. 95–302, doi:10.2475/05.2006.01.

Berner, R. A., and Schott, J., 1982, Mechanism of pyroxene and amphibole weathering—II. Observations of soil grains: American Journal of Science, v. 282, p. 1214–1231.

Berner, R. A., Sjöberg, E. L., Velbel, M. A., and Krom, M. D., 1980, Dissolution of Pyroxenes and Amphiboles during Weathering: Science, v. 207, p. 1205–1206, doi:10.1126/science.207.4436.1205.

Blum, A. E., and Stillings, L. L., 1995, Feldspar dissolution kinetics, *in* White, A. F., and Brantley, S. L., editors, Chemical Weathering Rates of Silicate Minerals: Mineralogical Society of America, Reviews in Mineralogy, v. 31, p. 291–351.

Boulangé, B., 1984, Les formations bauxitiques latéritiques de Côte-d'Ivoire: Travaux et Documents de l'ORSTOM, n. 175, 363 p.

——— 1987, Relation between lateritic bauxitization and evolution of landscape: Travaux ISCOBA, v. 16–17, p. 155–162.

Brantley, S. L., and Chen, Y., 1995, Chemical weathering rates of pyroxenes and amphiboles, *in* White, A. F., and Brantley, S. L., editors, Chemical Weathering Rates of Silicate Minerals: Mineralogical Society of America, Reviews in Mineralogy, v. 31, p. 119–172.

Bricker, O. P., 1986, Geochemical investigations of selected Eastern United States watersheds affected by acid deposition: Journal of the Geological Society, London, v. 143, p. 621–626, doi:10.1144/gsjgs.143.4.0621.

Bricker, O. P., and Rice, K. C., 1989, Acidic deposition to streams: Environmental Science & Technology, v. 23, p. 379–385, doi:10.1021/es00181a001.

Cole, W. F., and Lancucki, C. J., 1976, Montmorillonite pseudomorphs after amphibole from Melbourne, Australia: Clays and Clay Minerals, v. 24, p. 79–83, doi:10.1346/CCMN.1976.0240205.

Colin, F., ms, 1984, Étude pétrologique des altérations de pyroxénite du gisement nickélifère de Niquelandia (Brèsil): Université Paris, VII, Thèse, 137 p.

Colin, F., Noack, Y., Trescases, J.-J., and Nahon, D., 1985, L'altération latérique débutante des pyroxénites de Jacuba, Niquelandia, Brésil: Clay Minerals, v. 20, p. 93–113, doi:10.1180/claymin.1985.020.1.08.

Colin, F., Nahon, D., Trescases, J. J., and Melfi, A. J., 1990, Lateritic Weathering of Pyroxenites at Niquelandia, Goias, Brazil: The Supergene Behavior of Nickel: Economic Geology, v. 85, p. 1010–1023, doi:10.2113/gsecongeo.85.5.1010.

Delvigne, J., 1983, Micromorphology of the alteration and weathering of pyroxenes in the Koua Bocca ultramafic intrusion, Ivory Coast, West Africa, *in* Nahon, D., and Noack, Y., editors Pétrologie des Altérations et des Sols, Volume II: Strasbourg, Sciences Géologiques, Mémoires, v. 72, p. 57–68.

——— 1990, Hypogene and supergene alterations of orthopyroxene in the Koua Bocca ultramafic intrusion, Ivory Coast: Chemical Geology, v. 84, p. 49–53, doi:10.1016/0009-2541(90)90161-Y.

——— 1998, Atlas of Micromorphology of Mineral Alteration and Weathering: The Canadian Mineralogist, Special Publication 3, 495 p.
Dethier, D. P., 1988, A hydrogeochemical model for stream chemistry, Cascade Range, Washington, U.S.A.: Earth Surface Processes and Landforms, v. 13, p. 321–333, doi:10.1002/esp.3290130405.
Dixon, J. B., 1978, X-ray diffraction analysis, *in* Barnhisel, R. I., editor, Analyses of Clay, Silt and Sand Fractions of Selected Soils from Southeastern United States: Southern Cooperative Extension Series Bulletin, n. 219, p. 11–22.
Drever, J. I., 1973, The preparation of oriented clay mineral specimens for X-ray diffraction analysis by a filter-membrane peel technique: American Mineralogist, v. 58, p. 553–554.
Drever, J. I., and Hurcomb, D. R., 1986, Neutralization of atmospheric acidity by chemical weathering in an alpine drainage basin in the North Cascade Mountains: Geology, v. 14, p. 221–224, doi:10.1130/00917613(1986)14⟨221:NOAABC⟩2.0.CO;2.
Duchaufour, P., 1982, Pedology, (T. R. Paton, translator): London, George Allen and Unwin, 448 p.
Eggleton, R. A., 1975, Nontronite Topotaxial after Hedenbergite: American Mineralogist, v. 60, p. 1063–1068.
——— 1986, The relations between crystal structure and silicate weathering rates, *in* Colman, S. M., and Dethier, D. P., editors, Rates of Chemical Weathering of Rocks and Minerals: Orlando, Florida, Academic Press, p. 21–40.
Eggleton, R. A., and Boland, J. N., 1982, Weathering of enstatite to talc through a sequence of transitional phases: Clays and Clay Minerals, v. 30, p. 11–20, doi:10.1346/CCMN.1982.0300102.
Eslinger, E., and Pevear, D., 1988, Clay Minerals for Petroleum Geologists and Engineers: Society of Economic Paleontologists and Mineralogists, Short Course Notes 22, 422 p.
Gardner, L. R., 1992, Long-term isovolumetric leaching of aluminum from rocks during weathering: Implications for the genesis of saprolite: Catena, v. 19, p. 521–537, doi:10.1016/0341-8162(92)90051-C.
Goldich, S. S., 1938, A Study in Rock Weathering: The Journal of Geology, v. 46, p. 17–58, doi:10.1086/624619.
Hatcher, R. D., Jr., 1976, Introduction to the Geology of the Eastern Blue Ridge of the Carolinas and nearby Georgia: Carolina Geological Society Field Trip Guidebook, 53 p.
Hatcher, R. D., Jr., Hooper, R. J., Petty, S. M., and Willis, J. D., 1984, Structure and chemical petrology of three southern Appalachian mafic-ultramafic complexes and their bearing upon the tectonics of emplacement and origin of Appalachian ultramafic bodies: American Journal of Science, v. 284, p. 484–506.
Hatcher, R. D., Jr., Merschat, A. J., and Thigpen, J. R., 2005, Blue Ridge Primer, *in* Hatcher, R. D., Jr., and Merschat, A. J., editors, Blue Ridge Geology Geotraverse East of the Great Smoky Mountains National Park Western North Carolina: Carolina Geological Society Annual Field Trip Guidebook, p. 1–24.
Hawthorne, F. C., and Oberti, R., 2007, Classification of the Amphiboles, *in* Hawthorne, F. C., Oberti, R., Della Ventura, G., and Mottana, A., editors, Amphiboles: Crystal Chemistry, Occurrence, and Health Issues: Reviews in Mineralogy and Geochemistry, v. 67, p. 55–88, doi: 10.2138/rmg.2007.67.2.
Helms, T. S., McSween, H. Y., Jr., Labotka, T. C., and Jarosewich, E., 1987, Petrology of a Georgia Blue Ridge amphibolite unit with hornblende + gedrite + kyanite + staurolite: American Mineralogist, v. 72, p. 1086–1096.
Hornung, M., Adamson, J. K., Reynolds, B., and Stevens, P. A., 1986, Influence of mineral weathering and catchment hydrology on drainage water chemistry in three upland sites in England and Wales: Journal of the Geological Society, London, v. 143, p. 627–634, doi:10.1144/gsjgs.143.4.0627.
Katz, B. G., 1989, Influence of mineral weathering reactions on the chemical composition of soil water, springs, and groundwater, Catoctin Mountains, Maryland: Hydrological Processes, v. 3, p. 185–202, doi:10.1002/hyp.3360030207.
Katz, B. G., Bricker, O. P., and Kennedy, M. M., 1985, Geochemical mass-balance relationships for selected ions in precipitation and stream water, Catoctin Mountains, Maryland: American Journal of Science, v. 285, p. 931–962.
Keller, W. D., Reynolds, R. C., and Inoue, A., 1986, Morphology of clay minerals in the smectite-to-illite conversion series by scanning electron microscopy: Clays and Clay Minerals, v. 34, p. 187–197, doi: 10.1346/CCMN.1986.0340209
Klein, C., 2002, Manual of Mineral Science (22nd edition): New York, New York, John Wiley and Sons, 641 p.
Kretz, R., 1983, Symbols for rock-forming minerals: American Mineralogist, v. 68, p. 277–279.
Lerman, A., Wu, L., and Mackenzie, F. T., 2007, CO_2 and H_2SO_4 consumption in weathering and material transport to the ocean, and their role in the global carbon balance: Marine Chemistry, v. 106, p. 326–350, doi:10.1016/j.marchem.2006.04.004.
McSween, H. Y., Jr., and Hatcher, R. D., Jr., 1985, Field Trip #4: Ophiolites(?) of the Southern Appalachian Blue Ridge, *in* Woodward, N. B., editor, Field Trips in the Southern Appalachians: University of Tennessee Department of Geological Sciences, Studies in Geology 9, p. 144–170.
Miller, W. R., and Drever, J. I., 1977, Chemical weathering and related controls on surface water chemistry in the Absaroka Mountains, Wyoming: Geochimica et Cosmochimica Acta, v. 41, p. 1693–1702, doi:10.1016/0016-7037(77)90201-0.
Nahon, D. B., 1991, Introduction to the Petrology of Soils and Chemical Weathering: New York, John Wiley and Sons, 313 p.
Nahon, D. B., and Colin, F., 1982, Chemical weathering of orthopyroxenes under lateritic conditions: American Journal of Science, v. 282, p. 1232–1243.
Nahon, D., Colin, F., and Tardy, Y., 1982, Formation and distribution of Mg, Fe, Mn-smectites in the first stages of the lateritic weathering of forsterite and tephroite: Clay Minerals, v. 17, p. 339–348, doi:10.1180/claymin.1982.017.3.06.

Newton, R. M., and April, R. A., 1982, Surficial geological controls on the sensitivity of two Adirondack lakes to acidification: Northeastern Environmental Sciences, v. 1, p. 143–150.
O'Brien, A. K., Rice, K. C., Bricker, O. P., Kennedy, M. M., and Anderson, R. T., 1997, Use of geochemical mass balance modelling to evaluate the role of weathering in determining stream chemistry in five mid-Atlantic watersheds on different lithologies: Hydrological Processes, v. 11, p. 719–744, doi:10.1002/(SICI)1099-1085(199706)11:7⟨719::AID-HYP522⟩3.0.CO;2-2.
Ogg, C. M., and Smith, B. R., 1993, Mineral transformations in Carolina Blue Ridge-Piedmont soils weathered from ultramafic rocks: Soil Science Society of America Journal, v. 57, p. 461–472.
Plaster, R. W., and Sherwood, W. C., 1971, Bedrock weathering and residual soil formation in Central Virginia: Geological Society of America Bulletin, v. 82, p. 2813–2826, doi:10.1130/0016-7606(1971)82[2813:BWARSF]2.0.CO;2.
Price, J. R., Velbel, M. A., and Patino, L. C., 2005, Rates and timescales of clay-mineral formation by weathering in saprolitic regoliths of southern Appalachian Mountains from geochemical mass balance: Geological Society of America Bulletin, v. 117, n. 5, p. 783–794, doi:10.1130/B25547.1.
Proust, D., 1982, Supergene alteration of hornblende in an amphibolite from Massif Central, France, *in* van Olphen, H., and Veniale, F., editors, 7th International Clay Conference, Bologna and Pavia, 1981: Amsterdam, Elsevier Developments in Sedimentology 35, p. 357–364.
——— 1985, Amphibole weathering in a glaucophane-schist (Ile de Groix, Morbihan, France): Clay Minerals, v. 20, p. 161–170, doi:10.1180/claymin.1985.020.2.01.
Proust, D., Caillaud, J., and Fontaine, C., 2006, Clay minerals in early amphibole weathering: Tri- to dioctahedral sequence as a function of crystallization sites in the amphibole: Clays and Clay Minerals, v. 54, p. 351–362, doi:10.1346/CCMN.2006.0540306.
Psenner, R., 1989, Chemistry of high mountain lakes in siliceous catchments of the Central Eastern Alps: Aquatic Sciences, v. 51, p. 108–128, doi:10.1007/BF00879298.
Pundsack, F. L., 1956, Density and structure of endellite: Clays and Clay Minerals, v. 5, p. 129–135, doi:10.1346/CCMN.1956.0050110.
Rice, K. C., and Bricker, O. P., 1995, Seasonal cycles of dissolved constituents in streamwater in two forested catchments in the mid-Atlantic region of the eastern USA: Journal of Hydrology, v. 170, p. 137–158, doi:10.1016/0022-1694(95)92713-N.
Rice, T. J., Jr., Buol, S. W., and Weed, S. B., 1985, Soil-saprolite profiles derived from mafic rocks of the North Carolina Piedmont: I. Chemical, morphological, and mineralogical characteristics and transformations: Soil Science Society of America Journal, v. 49, p. 171–178.
Rochette, E. A., Drever, J. I., and Sanders, F. S., 1988, Chemical weathering in the West Glacier Lake drainage basin, Snowy Range, Wyoming: implications for future acid deposition: The University of Wyoming, Contributions to Geology, v. 26, p. 29–44.
Rolfe, B. N., 1953, Mineralogy of soil profiles: Iredell and Durham soils from the Piedmont Province of North Carolina: Clays and Clay Minerals, v. 2, p. 183–189, doi:10.1346/CCMN.1953.0020116.
Schroeder, P. A., Melear, N. D., West. L. T., and Hamilton, D. A., 2000, Meta-gabbro weathering in the Georgia Piedmont, USA: implications for global silicate weathering rates: Chemical Geology, v. 163, p. 235–245, doi:10.1016/S0009-2541(99)00129-1.
Smyth, J. R., and Bish, D. L., 1988, Crystal Structures and Cation Sites of the Rock-Forming Minerals: Boston, Massachusetts, Allen & Unwin, 332 p.
Stauffer, R. E., 1990a, Granite weathering and the sensitivity of alpine lakes to acid deposition: Limnology and Oceanography, v. 35, p. 1112–1134.
——— 1990b, Controls on surface water chemistry in the southern Blue Ridge and Piedmont provinces: Water, Air, and Soil Pollution, v. 52, p. 79–96, doi:10.1007/BF00283116.
Tardy, Y., 1971, Characterization of the principal weathering types by the geochemistry of waters from some European and African Crystalline massifs: Chemical Geology, v. 7, p. 253–271, doi:10.1016/0009-2541(71)90011-8.
Taylor, A. B., and Velbel, M. A., 1991, Geochemical mass balances and weathering rates in forested watersheds of the southern Blue Ridge. II. Effects of botanical uptake terms, *in* Pavich, M. J., editor, Weathering of Soils: Geoderma, v. 51, p. 29–50, doi:10.1016/0016-7061(91)90065-2.
Taylor, G., and Eggleton, R. A., 2001, Regolith Geology and Geomorphology: New York, New York, Wiley, 375 p.
Velbel, M. A., 1983, A dissolution-reprecipitation mechanism for the pseudomorphous replacement of plagioclase feldspars by clay minerals during weathering, *in* Nahon, D., and Noack, Y., editors, Pétrologie des Altérations et des Sols, Volume I: Strasbourg, Sciences Géologiques, Mémoires, v. 71, p. 139–147.
——— 1984, Natural weathering mechanisms of almandine garnet: Geology, v. 12, p. 631–634, doi:10.1130/0091-7613(1984)12⟨631:NWMOAG⟩2.0.CO;2.
——— 1985a, Geochemical mass balances and weathering rates in forested watersheds of the southern Blue Ridge: American Journal of Science, v. 285, p. 904–930.
——— 1985b, Hydrogeochemical constraints on mass balances in forested watersheds of the southern Appalachians, *in* Drever, J. I., editor, The Chemistry of Weathering: Holland, D. Reidel, p. 231–247.
——— 1989, Weathering of hornblende to ferruginous products by a dissolution-reprecipitation mechanism: Petrography and stoichiometry: Clays and Clay Minerals, v. 37, p. 515–524, doi:10.1346/CCMN.1989.0370603.
——— 1990, Mechanisms of saprolitization, isovolumetric weathering, and pseudomorphous replacement during rock weathering—A review: Chemical Geology, v. 84, p. 17–18, doi:10.1016/0009-2541(90)90149-2.
——— 1992, Geochemical mass balances and weathering rates in forested watersheds of the southern Blue

Ridge. III. Cation budgets and the weathering rate of amphibole: American Journal of Science, v. 292, p. 58–78.
——— 1993a, Formation of protective surface layers during silicate-mineral weathering under well-leached, oxidizing conditions: American Mineralogist, v. 78, p. 405–417.
——— 1993b, Weathering and pedogenesis at the watershed scale: Some recent lessons from studies of acid-deposition effects: Chemical Geology, v. 107, p. 337–339, doi:10.1016/0009-2541(93)90204-V.
——— 1999, Bond strength and the relative weathering rates of simple orthosilicates: American Journal of Science, v. 299 (Berner volume), p. 679–696.
——— 2004, Laboratory and Homework Exercises in the Geochemical Kinetics of Mineral-Water Reaction: Rate Law, Arrhenius Activation Energy, and the Rate-Determining Step in the Dissolution of Halite: Journal of Geoscience Education, v. 52, p. 52–59.
——— 2007, Surface Textures and Dissolution Processes of Heavy Minerals in the Sedimentary Cycle: Examples from Pyroxenes and Amphiboles, *in* Mange, M., and Wright, D., editors, Heavy Minerals in Use: Developments in Sedimentology v. 58, p. 113–150, doi:10.1016/S0070-4571(07)58004-0.
Velbel, M. A., and Barker, W. W., 2008, Pyroxene weathering to smectite: Conventional and cryo-field emission scanning electron microscopy, Koua Bocca ultramafic complex, Ivory Coast: Clays and Clay Minerals, v. 56, p. 111–126, doi:10.1346/CCMN.2008.0560110.
Velbel, M. A., Basso, C. L., Jr., and Zieg, M. J., 1996, The natural weathering of staurolite: Crystal-surface textures, relative stability, and the rate-determining step: American Journal of Science, v. 296, p. 453–472.
Velbel, M. A., McGuire, J. T., and Madden, A. S., 2007, Scanning electron microscopy of garnet from southern Michigan soils: Etching rates and inheritance of pre-glacial and pre-pedogenic grain-surface textures, *in* Mange, M., and Wright, D., editors, Heavy Minerals in Use: Developments in Sedimentology v. 58, p. 413–432, doi:10.1016/S0070-4571(07)58015-5.
White, A. F., 1995, Chemical weathering rates of silicate minerals in soils, *in* White, A. F., and Brantley, S. L., editors, Chemical Weathering Rates of Silicate Minerals: Mineralogical Society of America, Reviews in Mineralogy, v. 31, p. 407–461.
——— 2005, Natural weathering rates of silicate minerals, *in* Drever, J. I., editor, Surface and Ground Water, Weathering, and Soils: Oxford, Elsevier-Pergamon, Treatise on Geochemistry, v. 5, p. 133–168, doi: 10.1016/B0-08-043751-6/05076-3.
White, A. F., Blum, A. E., Schulz, M. S., Vivit, D. V., Stonestrom, D. A., Larsen, M., Murphy, S. F., and Eberl, D., 1998, Chemical weathering in a tropical watershed, Luquillo Mountains, Puerto Rico: I. Long-term versus short-term weathering fluxes: Geochimica et Cosmochimica Acta, v. 62, p. 209–226, doi:10.1016/S0016-7037(97)00335-9.
Wicks, F. J., and Whittaker, E. J. W., 1977, Serpentine textures and serpentinization: Canadian Mineralogist, v. 15, p. 459–488.
Wilson, M. J., 2004, Weathering of the primary rock-forming minerals: processes, products and rates: Clay Minerals, v. 39, p. 233–266, doi:10.1180/0009855043930133.